1-12-2016

Identifying Axonal Injury in Cervical Facet Joint Capsules as a Result of High-Rate Tensile Stretch in an In-vivo Goat Model

Christopher Stuart Shaw
University of Windsor

Identifying Axonal Injury in Cervical Facet Joint Capsules as a Result of High-Rate Tensile Stretch in an In-vivo Goat Model

By

Christopher Shaw

A Thesis
Submitted to the Faculty of Graduate Studies
through the Department of Kinesiology
in Partial Fulfillment of the Requirements for
the Degree of Master of Human Kinetics
at the University of Windsor

Windsor, Ontario, Canada

2016

Identifying Axonal Injury in Cervical Facet Joint Capsules as a Result of High-Rate Tensile Stretch in an In-vivo Goat Model

by

Christopher Shaw

APPROVED BY:

_____

Dr. Barbara Zielinski
Department of Biological Sciences

_____

Dr. Kevin Milne
Department of Kinesiology

_____

Dr. Nadia Azar, Advisor
Department of Kinesiology

December 16, 2015

AUTHOR'S DECLARATION OF ORIGINALITY

I hereby certify that I am the sole author of this thesis and that no part of this thesis has been published or submitted for publication.

I certify that, to the best of my knowledge, my thesis does not infringe upon anyone's copyright nor violate any proprietary rights and that any ideas, techniques, quotations, or any other material from the work of other people included in my thesis, published or otherwise, are fully acknowledged in accordance with the standard referencing practices. Furthermore, to the extent that I have included copyrighted material that surpasses the bounds of fair dealing within the meaning of the Canada Copyright Act, I certify that I have obtained a written permission from the copyright owner(s) to include such material(s) in my thesis and have included copies of such copyright clearances to my appendix.

I declare that this is a true copy of my thesis, including any final revisions, as approved by my thesis committee and the Graduate Studies office, and that this thesis has not been submitted for a higher degree to any other University or Institution.

ABSTRACT

This study investigated the presence of axonal injury within cervical facet joint capsules (FJC) exposed to a high-rate (100 mm/s) tensile stretch. The left C5-C6 FJCs of five anaesthetized goats were subjected to a series of tensile tests in 4 mm increments until rupture (the intact right FJCs served as controls). The FJCs were harvested, fixed in 4% buffered paraformaldehyde, embedded in paraffin, and serially sectioned. FJC sections were immunolabeled for neurofilament light chain (NF-L) and beta-amyloid precursor protein (β-APP). A significantly higher frequency of coupled β-APP/NF-L immunoreactive sections was found in stretched (23.8%) compared to unstretched FJCs (6.3%, $p = 0.02$). This finding suggests that high-rate tensile stretch is a mechanism for axonal injury in cervical FJCs, and furthers the understanding of axonal injury in the whiplash pain mechanism. The use of the dual immunolabeling, presents a new method for identifying axonal injury in skeletal tissue.

ACKNOWLEDGEMENTS

I would first like to thank Dr. Srinivasu Kallakuri, Dr. John Cavanaugh and the rest of the Wayne State University spine research group for allowing me to use their facilities and equipment throughout the duration of this thesis project. Dr. Kallakuri is also deserving of more gratitude for his ever-present guidance, technical help, and wisdom in many aspects of my experience in the spine research laboratory. In addition, my peers in the lab group created a very positive and engaging experience for me.

I would also like to thank Dr. Barbara Zielinski and Dr. Kevin Milne for being on my thesis committee. The insight and guidance from different perspectives was gladly acknowledged and incorporated, which ultimately strengthened the entire project.

Extending thanks to my family and friends, for their ongoing support throughout this long journey. All have provided balance in my life during this project, from keeping me from delving too deep into my work and help me enjoy the moment, to motivating me and creating an environment where I could work at my best. For this, I thank you all.

Last, and certainly not least, I would like to thank my advisor Dr. Nadia Azar. From the beginning where she accepted me as a graduate student all the way to the end where I stand now, Nadia helped me immensely throughout this project. From guidance in choosing what kind of project to undertake, and supporting me through every step till completion. For everything you have done, thank you.

TABLE OF CONTENTS

LIST OF TABLES

LIST OF FIGURES

LIST OF APPENDICES

LIST OF ABBREVIATIONS/SYMBOLS

1°: Primary antibody

2°: Secondary antibody

β-APP: Beta-amyloid precursor protein

ABC: Avidin biotin complex

ACC: Animal care committee

ALL: Anterior longitudinal ligament

BiP: Binding protein

C1-C7: Cervical vertebrae 1-7

CGRP: Calcitonin gene-related peptide

DPX: Distyrene plasticizer xylene

EAAC1: Excitatory amino acid carrier 1

FJC: Facet joint capsule

IACUC: Institutional animal care and use committee

IM: Intramuscular

IV: Intravenous

IHC: Immunohistochemistry

LF: Ligamentum flavum

mGluR5: Metabotropic glutamate receptor 5

MVA: Motor vehicle accident

NF-L: Neurofilament light chain

PBS: Phosphate buffered saline

PLL: Posterior longitudinal ligament

SCM: Sternocleidomastoid

SP: Substance P

WAD: Whiplash-associated disorder

NOMENCLATURE

β-Amyloid precursor protein:	an integral membrane protein concentrated in the synapses of neurons; best known as the precursor molecule whose protein breakdown generates beta amyloid; a marker of neuronal injury (Gentleman et al., 1993).
Allodynia:	a particular case of hyperalgesia in which a stimulus that is usually not painful becomes noxious (Dong & Winkelstein, 2010)
Cineradiography:	the process of making radiographs of moving objects in sufficiently rapid sequence so that the radiographs may be projected as motion pictures (Kaneoka et al., 1999).
Contralateral:	relating to or denoting the side of the body opposite to that on which a particular structure or condition occurs.
Endogenous:	produced or caused by factors within the organism, tissue, or system (Burry, 2010).
Hyperalgesia:	an increased response to a stimulus that is normally painful, and includes all conditions of increased pain sensitivity (Dong & Winkelstein, 2010).
Immunoreactivity:	the reaction between an antigen and its respective antibody (Burry, 2010).
Ipsilateral:	belonging to or occurring on the same side of the body.
Morphology:	the branch of biology dealing with the study of the form and structure of organisms and their specific structural features (Kallakuri et al., 2008).
Neurofilament light chain:	a component of the neuronal cytoskeleton, composed of polypeptide chains that provide structural support of the axon and help regulate axon diameter (Friede & Samorajski, 1970).
Noxious:	harmful, causing pain.

CHAPTER 1

Introduction

Neck pain is common in in today's society with annual incidence rates ranging from 30-50% in the general population, and a lifetime prevalence rate approaching 70% (Bogduk, 1999a; Hogg-Johnson et al., 2008). Neck pain is assumed to be a multifactorial condition with many different causes, one of them being whiplash injuries (Ariëns, van Mechelen, Bongers, Bouter, & van der Wal, 2000). The whiplash mechanism can be defined as "a rapid acceleration-deceleration mechanism of energy transferred to the neck that results in soft tissue injury…" (Holm et al., 2008). The clinical entities arising from the injury have been termed whiplash-associated disorder (WAD) by the Québec Task Force on Whiplash-Associated Disorders (Holm et al., 2008). This definition was adopted in order to distinguish the whiplash injury mechanism from the disorders the mechanism can create. Kaneoka, Ono, Inami, & Hayashi (1999) describe the whiplash mechanism as the trunk being pushed upward into the neck. The initial forward motion of the lower vertebrae relative to the upper vertebrae (which lag behind) creates an "S"-shape in the cervical spine.

The prevalence of WAD varies by geographical location, however the annual prevalence rate in North America and western Europe is approximately 300 per 100 000 population (Barnsley, Lord, & Bogduk, 1994; Holm et al., 2008). Over the past 30 years there has been a continual, unexplained increase in reported WAD, which in turn adds to the rising cost and burden on society (Holm et al., 2008). The majority of whiplash injuries occur in motor vehicle accidents (MVA), and when that is the case there is often a litigation process, insurance claims, and required medical attention. In 1996, Canada

spent $600 million (CAD) for whiplash-related claims in British Columbia alone (Navin, Zein, & Felipe, 2000). Harder, Veilleux, & Suissa (1998) reported that in Canada, 43% of the total cost is generated by only 12% of patients – those with more than 6 months of compensation time. Of the population who experience a MVA, it is noted that up to 20% will develop WAD, of those 14-42% will progress to develop chronic symptoms (Barnsley et al., 1994; Gargan & Bannister, 1994; Stovner, 1996).

Many anatomical structures are subject to damage/deformation in whiplash injuries, including the vertebral arteries, spinal ganglia nerve cells, neck muscles, anterior longitudinal ligaments, intervertebral discs and facet joint capsules (FJCs) (Curatolo et al., 2011). The bulk of the literature has focused on FJCs, and many convergent lines of evidence support the FJCs as a significant contributor to pain in people who have experienced a whiplash injury (Bogduk, 1999a). The FJCs are innervated via the medial branch of the dorsal ramus, and contain both mechanoreceptors and pain sensing neural fibres (Bogduk, 1982; Kallakuri, Singh, Chen, Cavanaugh, 2004). Mechanical testing with cadaver specimens has established the strain limits of the FJC and support excessive tensile stretch as a prominent mechanism of injury (Panjabi et al., 1998; Winkelstein et al., 2000; Cusick, Pintar, Yoganandan, 2001; Pearson, Ivancic, Ito, & Panjabi, 2004). Kinematic studies using human volunteers have been performed to examine the impact of muscle activity on spine kinematics in whiplash scenarios (Kaneoka et al., 1999; Siegmund et al., 2003). Neurophysiologic studies using in-vivo animal models have demonstrated activation of neural elements involved in signaling pain as a result of FJC stretch, as well as persistent discharges from these neural elements after non-physiologic FJC stretch which could potentially elicit sustained pain (Lu, Chen, Kallakuri,

Patwardhan, & Cavanaugh, 2005b). Behavioural studies using similar models have also demonstrated persistent pain from the same mechanism in the form of overt pain behaviours (e.g., withdrawal response upon forepaw stimulation: Lee, Thinnes, Gokhin, & Winkelstein, 2004; Quinn, Lee, Ahaghotu, &Winkelstein et al., 2007; Winkelstein & Santos, 2008), which were correlated with spinal glial cell activation (Winkelstein & Santos, 2008) and exaggerated firing response of dorsal horn neurons (Quinn et al., 2010).

As previously mentioned, pain sensing fibres exist in the FJC, and the intention of nociceptive pain is to protect the tissue (Winkelstein, 2011). These fibres should only fire in the presence of a noxious stimuli; however, damaged nociceptors may become sensitized, thus increasing their firing rate or lowering their threshold for firing (Kawakami et al., 2003; Rothman & Winkelstein, 2007; Winkelstein, 2011). There are cases where axons of neurofibres become extensively damaged and cannot be repaired, thus two distinct phases of axon injury have been identified. Primary axotomy involves the disruption of the axon cylinder, and the secondary axotomy is where progressive alterations of the cylinder take place (Povlishock & Christman, 1995). These alterations include axon swellings, terminal retraction balls, and in some cases excessively knotty, wrinkled appearances (Kallakuri et al., 2008).

An effective and reliable way method to visualize neurons throughout peripheral tissue is through immunohistochemistry, a process where antibodies are employed for their highly specific binding to desired amino acid sequences (Burry, 2010; Friede & Samorajski, 1970; Schwartz, Hua, Cañete-Soler, & Schlaepfer, 1998; Van Geel, Rosengren, & Verbeek, 2005). Antibodies to neurofilament light chain (NF-L: integral

components of the axon cytoskeleton that maintain diameter and rate of conduction) have been used to visualize axons within different types of tissue such as brain, optic tissue and facet joint capsules, and even as a marker for axonal injury through the examination of axon morphology (Friede & Samorajski, 1970; Grady et al., 1993; Dräger & Hofbauer, 1984; Kallakuri, Li, Chen, & Cavanaugh, 2012; Meller, Bellander, Schmidt-Kastner & Ingvar, 1993; Schwarz et al., 1998; Van Geel et al., 2005). In addition to NF-L, immunolabeling for antibodies against beta-amyloid precursor protein (β-APP) has also been widely used to detect diffuse axonal injury (An et al. 1997; Gentleman, Nash, Sweeting, Graham, & Roberts, 1993; Hayashi, Ago, Ago, & Ogata, 2009; Sherriff et al. 1994a; Sherriff, Bridges, & Sivaloganathan, 1994b; Uryu et al., 2007). β-APP is a membrane spanning glycoprotein in neuronal cells whose functions are thought to include cell adhesion, growth and, importantly, response to injury (Sherriff et al., 1994b). In the event of axonal breakdown, β-APP accumulation occurs (a process that requires energy and thus can only occur while there is still life) and reaches detectable levels within 3 hours post-injury (Sherriff et al., 1994a, 1994b; Uryu et al., 2007). This highlights the strength of using β-APP immunolabeling in addition to NF-L immunolabeling – not only are axons being identified (NF-L), but injured axons are distinguished from normal ones (β-APP).

Kallakuri et al. (2008) demonstrated the presence of altered axon morphologies following low-rate, non-physiologic tensile stretch of goat cervical FJCs. For a number of reasons, the majority of studies that replicate whiplash injuries in in-vivo models (both animal and human) have applied the whiplash exposure at a low rate. Participant safety in human volunteer studies, and minimizing the risk of accidentally rupturing the FJC or

stretching it beyond its physiologic range are some reasons why many studies have applied a low rate of FJC stretch. The FJC stretch rate employed by Kallakuri et al. (2008) was only 0.5 mm/s, which represents stretch rates seen in neck motions of activities of daily living (Lu, Chen, Kallakuri, Patwardhan, & Cavanaugh, 2005c). In order to more accurately represent the conditions and loading that occur during a whiplash event, a high rate of FJC stretch is required.

Therefore, the purpose of the present study is to investigate the presence of axonal injury within FJCs exposed to high-rate stretch (100 mm/s). High-rate tensile stretch provides a better representation of the FJC stretch rates observed in simulations of higher speed rear-impact MVAs. Samples of stretched and unstretched goat FJCs were harvested from a series of experiments conducted at Wayne State University in 2007 (Azar et al., 2011). Paraffin-embedded sections of these samples were immunolabeled for NF-L and β-APP and examined under a light microscope for evidence of axonal injury through the accumulation of β-APP. It was hypothesized that there would be an increased amount of axonal injury in the stretched FJCs, compared to the unstretched FJCs from the same test subject.

CHAPTER 2

Review of Literature

2.1 Neck Anatomy

2.1.1 Cervical Vertebrae

The top seven vertebrae of the spine are the bones found in the neck; the cervical vertebrae (C1-C7) **(Figure 1)**. The cervical vertebrae allow for the widest range of motion compared to other sections of the vertebral column, largely due to the uniqueness of the top two vertebrae, the *atlas* (C1) and the *axis* (C2). Compared to the rest of the spine, cervical vertebrae have much more mobility at their joint surfaces, which adds to the broader range of motion of the neck, and are smaller than the vertebrae of the other spine regions because they do not support as much loading (Tortora & Nelsen, 2009). All vertebrae have *vertebral foramina* which house the spinal cord. The foramina's width and depth have been consistently shown to be at its largest at C2, remain constant from C3-

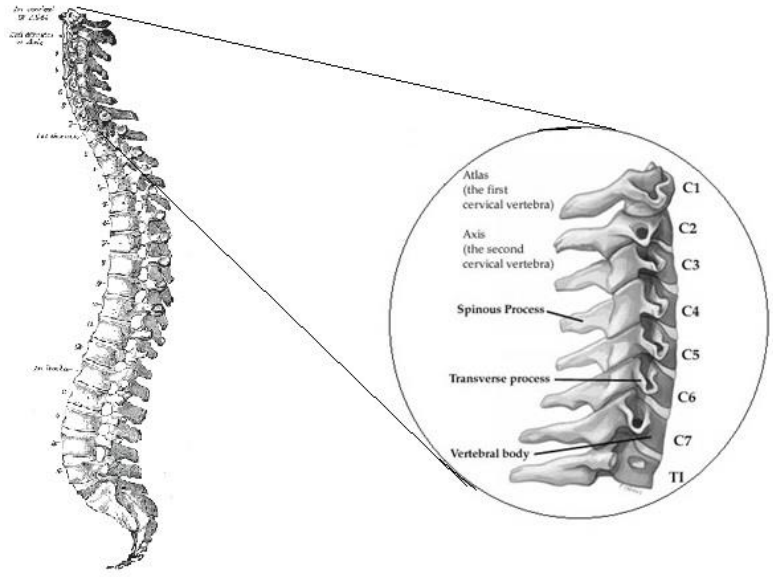

Figure 1: The vertebral column (left) and a close up of the cervical spine (right). (Images: left, Gray & Lewis, 2000, p. 25; right, http://www.hughston.com/hha/a.cspine.htm).

C6 and be slightly smaller at C7 (Panjabi, Duranceau, Goel, Oxland, & Takata, 1991a; Francis, 1955). The cervical vertebrae have the largest vertebral foramina because in the area, the spinal cord is at its thickest. Unique to cervical vertebrae are two *transverse foramina*, which are lateral to each side of the vertebrae on the transverse processes. Passing through these foramina are the vertebral artery, vertebral vein and cranial nerves (Tortora & Nelsen, 2009). As previously mentioned, the top two vertebrae are unique to all others. Atlas (C1) lacks a vertebral body and spinous process. It also has concave *superior articular facets* that articulate with the *occipital condyles* of the occipital bone, allowing a head-neck movement that signals "yes." Axis (C2) does have a body, however its defining feature is that it has a protruding process called the *dens,* which fits in nicely within the vertebral foramen of C1. This connection is called the *atlanto-axial joint* and allows for movement of the head that signals "no" (Tortora & Nelsen, 2009). The rest of the vertebrae are relatively similar to the initial description except for C7, or *vertebra prominens,* which has a larger spinous process that can be felt at the base of the neck (Panjabi et al., 1991a). The bottom 5 cervical vertebrae contact each other in the transverse plane through each of their superior and inferior articular facets, which allow for a variety of neck movements including lateral bending, flexion and extension, and neck rotation (Tortora & Nelsen, 2009).

2.1.2 Cervical Ligaments and Intervertebral Discs

Like other ligaments throughout the body, the cervical spine ligaments' main purpose is to restrict excessive vertebral movement. **Figure 2** shows a functional spinal unit with spinal ligaments. *Ligamentum flavum* (LF) ligaments lie in pairs on the laminae of each vertebra and are strong stabilizers (Aspden, 1992). LF's orientation is almost vertical, with the majority of its fibres running in the same direction. LF's width remains constant, however its length increases at each inferior vertebral level (Panjabi, Oxland & Parks, 1991b). The *anterior longitudinal ligament* (ALL) and the *posterior longitudinal ligament* (PLL) span the entire presacral spine (Panjabi et al., 1991b). Both ALL and PLL are tightly adhered to the vertebral bodies and intervertebral discs: ALL on the anterior side, PLL on the posterior side. In conjunction with the LF, PLL becomes stiffer when the spine is flexed forward whereas ALL becomes stiff when the spine is extended backward (Aspden, 1992). The *facet capsules* envelop the facet joint, spanning in the transverse plane from the inferior articular process of one vertebra to the superior

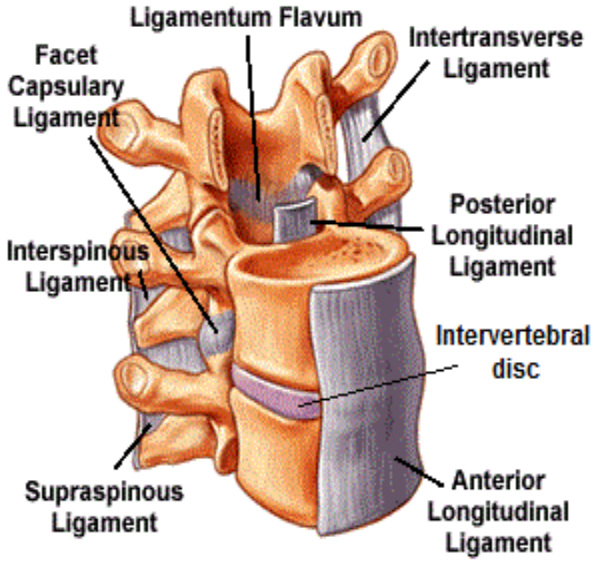

Figure 2: A functional spinal unit showing the ligaments and intervertebral disc. (Image: http://www.coloradospineinstitute.com/subject.php?pn=anatomy-ligaments-17).

articular process of the vertebra directly inferior to it. Facet capsular ligaments allow for, and restrict antero-posterior flexion and extension in the sagittal plane of the neck (Hamill & Knutzen, 2009). The *supraspinous ligament* and the *interspinous ligament* are both poorly developed in the cervical spine and do not strongly contribute to spinal stabilization (Panjabi, et al., 1991a). The fibres in between each of the vertebrae are cartilaginous intervertebral discs. Intervertebral discs are located between the vertebral bodies; they allow for some movement and bear the load of body parts superior to the disc's level (Tortora & Nelsen, 2009). The outer ring is mainly fibrous cartilage, called the *annulus fibrosis*, which surrounds the soft and highly elastic center called the *nucleus pulposus* (Tortora & Nelsen, 2009). These discs are mostly avascular and rely on the surrounding bodies of the vertebrae for a blood supply, in order to clear waste and deliver oxygen and nutrients (Tortora & Nelsen, 2009).

2.1.3 Cervical Musculature

The neck is comprised of many muscles (**Figure 3)**, at times recruiting over more than 20 pairs for stabilizing and movement purposes, with some muscles often spanning two or more joints (Kamibayashi & Richmond, 1998). Originating from the sternum and clavicle, and inserting at the mastoid process of the temporal bone the *sternocleidomastoid* (SCM) is the main head-neck flexor muscle (Tortora & Nelsen, 2009). Innervated by the *accessory (XI) nerve*, bilateral contraction of both SCM will flex the neck forward whereas when contracted unilaterally, the SCM causes the neck to laterally flex and rotate (Tortora & Nelsen, 2009). On the posterior side of the neck are the *capitis* group of muscles. All three sets are all innervated by *cervical spinal nerves* and insert in a similar area, either the occipital bone of the mastoid process. *Semispinalis*

capitis originates from the spinous processes of C7-T7 ("T" = thoracic vertebrae) and the articular processes of C4-C6; *spinalis capitis* arises from semispinalis capitis; *splenius capitis* originates from the ligamentum nuchae and the spinous processes of C7-T4; and *longissimus capitis* originates from the transverse processes of T1-T4 and the articular processes of C4-C7. When contracting bilaterally, these muscles will extend the neck posteriorly, and if contracted unilaterally will cause ipsilateral neck rotation (Tortora & Nelsen, 2009; Kamibayashi & Richmond, 1998). Another neck muscle group, the *cervicis* muscles, are also responsible for neck/spine extension when contracted bilaterally; however, when contracted unilaterally they create contralateral rotation. Like the capitis muscles, cervicis muscles are innervated by the cervical spinal nerves, as well

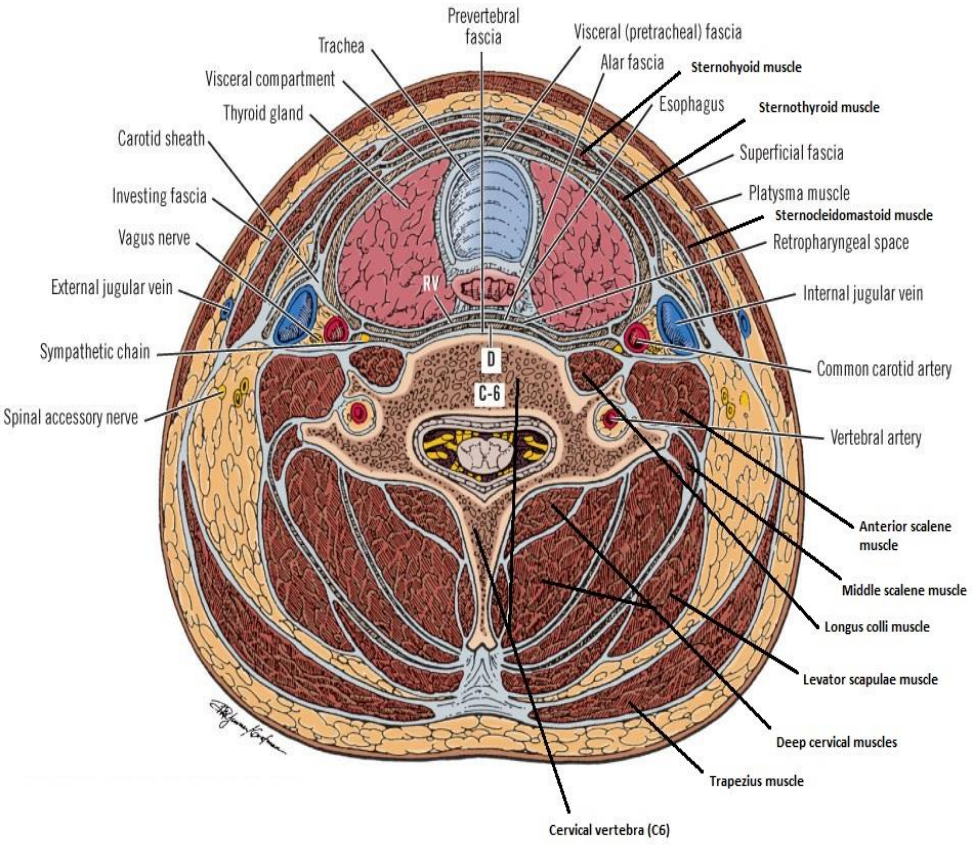

Figure 3: A cross-sectional view of the neck at C6 (Image: Adapted from Skandalakis et al., 2004, p. 272).

as some thoracic spinal nerves. *Semispinalis cervicis* originates from the transverse processes of T1-T5, *spinalis cervicis* originates from the ligamentum nuchae and spinous process of C7, *splenius cervicis* originates from spinous processes of T3-T6, *longissimus cervicis* originates from the transvers processes of T4-T5, and *iliocostalis cervicis* originates from ribs 1-6. Both spinalis cervicis and semispinalis cervicis insert to spinous processes of more superior vertebrae while the other three muscles insert into the transverse processes of more superior vertebrae (Tortora & Nelsen, 2009; Kamibayashi & Richmond, 1998). The *trapezius* muscle is the most superficial back/neck muscle, and covers a large area extending from the skull and vertebral column medially out to the pectoral girdle laterally. It originates from the superior nuchal line of the occipital bone, ligamentum nuchae, and the spinous processes of C7-T12; it inserts at the clavicle, acromion, and the spine of the scapula; and is innervated by accessory (XI) nerve and cervical spinal nerves (Tortora & Nelson, 2009). Due to it being so widespread, covering many angles of action, contraction of trapezius results in many motions, however for neck motion, it creates extension (Tortora & Nelsen, 2009). A number of other paraspinal muscles exist, such as the *multifidii* and *rotatores*, which originate and insert in between each vertebrae. Winkelstein et al. (2001) demonstrated that the insertion locations of these muscles were consistent throughout the cervical levels. When contracted, these muscles do not create any major motions; their main purpose is for spinal stabilization and restriction of any movement that may induce injury to surrounding tissues (Tortora & Nelsen, 2009).

2.1.4 Innervation

The cervical spine also houses a great deal of nervous tissue. Spinal nerves, and the subsequent nerves that branch off of them, are part of the peripheral nervous system, and connect all parts of the body to the central nervous system (spinal cord, and ultimately brain). Of the 31 pairs of spinal nerves, there are 8 pairs of cervical nerves (the cervical plexus: **Figure 4**). The first pair emerge from the between the occipital bone and atlas whereas the rest of the cervical nerves breach through intervertebral foramina of adjoining vertebrae (Schulte, Schuenke, & Schumacher, 2006; Tortora & Nelsen, 2009). Efferent nerves branch off the spinal cord anteriorly as small ventral rootlets that converge into ventral roots. Afferent nerves heading back to the spinal cord are contained in the dorsal roots that diverge into dorsal rootlets, joining the spinal cord posteriorly (Schulte, et al. 2006). Additionally, each dorsal root has a swelling filled with cell bodies of afferent nerves called the *dorsal root ganglion*. The dorsal and ventral roots then

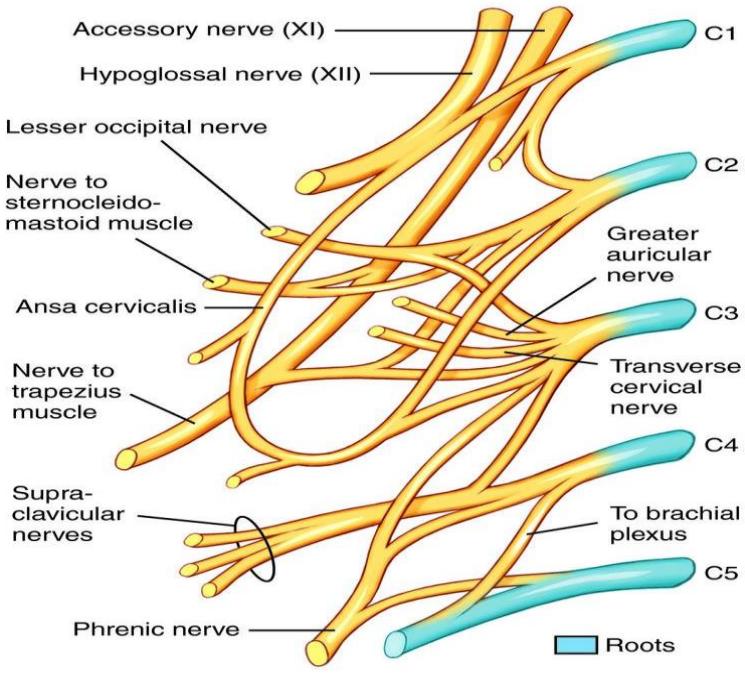

Figure 4: The cervical plexus. (Image: Mosby's dictionary of medicine, nursing & health professions, 2013, p. 331)

converge to create the spinal nerve trunk, containing a mixture of both sensory and motor neurons. These eventually branch off to ventral and dorsal rami, which set off to a variety of peripheries throughout the body (Tortora & Nelsen, 2009).

2.2 Whiplash Associated Disorders (WAD)

2.2.1 Epidemiology

Neck pain is a common occurrence in today's society, with annual incidence rates ranging from 30-50% in the general population, and a lifetime prevalence rate approaching 70% (Bogduk, 1999a; Hogg-Johnson et al., 2008). More severe neck pain, where activities of daily living are limited or restricted, have yearly prevalence rates as high as 11.5% (Hogg-Johnson et al., 2008). Once source of neck pain that merits noting is pain caused by a whiplash mechanism, which most commonly occurs in rear-impact MVAs, followed by less common occurrences in falls and other mishaps (Holm et al., 2008). The whiplash mechanism can be defined as "a rapid acceleration-deceleration mechanism of energy transferred to the neck that results in soft tissue injury…" (Holm et al., 2008). When an injury caused by whiplash occurs, the clinical entities related to the injury have been named whiplash-associated disorders (WAD) by the Québec Task Force on Whiplash-Associated Disorders (Holm et al., 2008). This definition was created in order distinguish the whiplash mechanism itself from the disorders that manifest from it (Holm et al., 2008).

The prevalence of WAD has been reviewed by many, but the most recent data suggests that the annual prevalence in North America and western Europe is likely to be at least 300 per 100 000 population (Holm et al., 2008). These rates coincide with a

continual increase in reported WAD cases over the past 30 years, but as yet there is no clear indication as to why the rates are increasing (Holm et al., 2008).

2.2.2 Recovery and Prognosis

Of those exposed to MVA Barnsley et al. (1994) suggested that up to 20% will develop symptoms in their neck. In most cases, patients with WAD will recover and be symptom free within the first three months post-injury; however, in 14-42% of cases, patients will progress to chronic symptoms (Barnsley et al., 1994; Gargan & Bannister, 1994; Stovner, 1996; Harder et al., 1998). Gargan & Bannister (1994) noted that if patients become asymptomatic within the first three months, they will likely not experience any more symptoms from the initial injury, however if symptoms do persist after 3 months, 86% of patients would have long recovery periods, remaining symptomatic for up to two years. Harder et al. (1998) found that if a patient experienced another injury in conjunction with WAD in a MVA, there would be an increased likelihood for chronic symptom development (alluding to a more serious MVA). However, the strongest prognostic determinant of chronic symptoms occurrence was the high initial pain intensity following a MVA (Scholten-Peeters et al., 2003).

2.2.3 Direct and Indirect Costs

Whenever an injury occurs and there is lost work time, a litigation process, and/or required medical attention, there are unavoidably going to be associated costs. In British Columbia alone, Canada spent $600 million (CAD) in 1996 for whiplash-related claims, representing 27% of the total claim cost incurred by the Insurance Corporation of British Columbia (Navin, Zein, & Felipe, 2000). In Canada, close to half of the cost for patients with WAD is generated by 12% of patients with more than 6 months of compensation

time (Harder et al., 1998). More recently, annual medical costs in the United States have been reported in the range of $356 million (USD) with a total cost projected at $3.9 billion (USD) (Winkelstein et al., 2000). With the majority of costs coming from the population who have extended recovery periods, the chronic nature of the symptoms is what generates the greatest amount of cost among those with whiplash injuries.

2.3 Whiplash Injury Mechanism

Early studies on whiplash describe the mechanism as involving flexion and extension of the neck (Bogduk, 1999a). However, research from the late 1990s revealed that this view was not quite correct (Panjabi et al., 1998; Kaneoka, et al., 1999; Bogduk, 1999a). Several studies have demonstrated that upon rear impact, the trunk is pushed upwards into the neck, creating a sigmoid (or "S")-shape in the cervical spine (Panjabi et al., 1998; Kaneoka, et al., 1999; Luan et al., 2000). At the same time, the trunk moves forward, but the head lags behind, resulting in an initial forward motion of the lower vertebral levels and lagging upper levels. This sigmoid deformation causes abnormal joint rotations that cause the lower vertebrae to spin backwards without any translation (**Figure 5**) (Bogduk, 1999b). The backwards rotation of the vertebrae creates separation of the anterior side of the two vertebral bodies while on the posterior side the moving vertebrae inferior articular process chisels into its supporting superior articular process. This motion precedes a number of issues that can arise, such as anterior tearing of the annulus fibrosis, contusion of the intra-articular meniscoids or impaction fractures of the articular processes within the zygapophysial (facet) joint (Bogduk, 1999a).

2.4 Structures Prone to Injury

There is evidence that shows that multiple structures within the neck that are subject to damage/deformation in whiplash injuries, such as threshold-exceeding strains to ligaments, ruptures of joint capsules, and intervertebral disc lesions (Curatolo et al., 2011), and these various structures share a role in contributing to symptoms of WAD. Eichberger, Darok, & Steffan (2000) hypothesized that the dorsal root ganglia may be injured due to rapid changes in pressure gradients (caused by rapid head-neck movement) in the spinal canal. Although surrounding vasculature aids in the maintenance of a pressure gradient, Svensson et al. (1998) demonstrated that these rapid gradient changes induce the breakdown of the plasma membranes of the spinal ganglia nerve cells. The vertebral artery is also subject to injury in a whiplash scenario. Šerić, Blažić-Čop, & Demarin (2000) showed signs of altered blood flow rates in arterial dissections of whiplash patient cadavers. In cadaveric spine sled tests, Panjabi et al. (1998) observed that vertebral artery elongation exceeded physiologic limits, suggesting lesions could

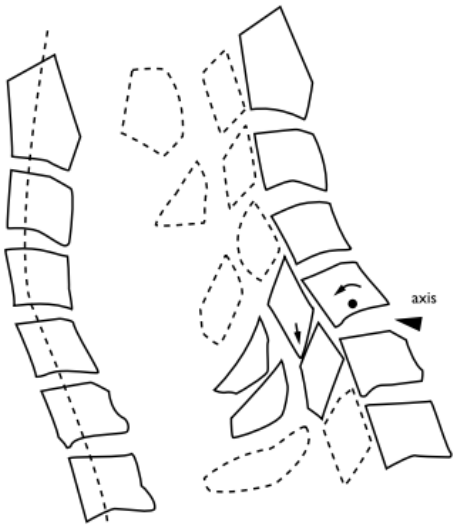

Figure 5: **Tracings of an X-ray of the cervical spine during a rear-end impact**. This image demonstrates the "S"-shaped distortion and a high axis of rotation, without translation of the vertebra. (Image: originally published in Kaneoka et al., 1999, p.767; adapted by Bogduk, 1999a, p.265)

occur. This injury typically originates from an intimal tear at the C1-C2 joint, and symptoms develop between 4-12 months after the MVA (Šerić et al., 2000; Chung & Han, 2002; Taneichi, Suda, Kajino, & Kaneda, 2005).

Similar to vertebral artery injury experimental procedures, research investigating the anterior longitudinal ligaments and intervertebral discs does not exist outside of post-mortem cadaver studies (Curatolo et al., 2011). In cadavers subjected to rear impacts, tears of the anterior longitudinal ligament and rim lesions of the anterior annulus fibrosis have been documented (Yoganandan, Cusick, Pintar, & Rao, 2001). Currently, there are no imaging techniques to demonstrate pain-provoking strains to the anterior disc *in vivo*, due to the fact research on these structures outside of post-mortem cadaver have not yet been explored. The structures are similar in composition to the posterior ligaments (such as facet joint capsules) which have been extensively observed, and theoretically should produce a similar physiological response (Curatolo et al., 2011). However, this has yet to be demonstrated empirically.

A considerable amount of research has investigated the neck muscles as sites of injury and causes of symptoms for WAD. The sternocleidomastoid, the trapezius and paraspinal muscles are commonly injured during whiplash (Fredin et al., 1997; Brault, Siegmund, & Wheeler, 2000; Gerdle et al., 2008). Neck muscles have been shown to undergo eccentric contraction during a whiplash motion, subjecting the muscles to potentially injurious strains (Brault et al., 2000; Vasavada, Brault, & Siegmund, 2007). The result of acute injury to the muscles exceeding their physiological stretch limits falls in line with what has been shown biochemically. Biochemical indicators of pain have been documented shortly after injury, within a range of 6-24 hours post injury (Evans et

al., 1986; Scott & Sanderson, 2002). Elevated levels of serum creatine kinase appear acutely following the whiplash event and typically return to normal levels by 48 hours post-injury (Scott & Sanderson, 2002). Of the literature focusing on neck pain symptoms, definitive answers on neck muscles being the root of the problem are scarce. Increased tension in neck muscles after whiplash injuries is likely due to damage within sensory structures of underlying tissues (e.g. ligaments, bones, etc.), further discrediting muscles as the major contributor to WAD symptoms (Fredin et al. 1997). The general consensus is that neck muscles are likely contributors to acute WAD symptoms, however for chronic symptoms, neck muscles are not seen to contribute, pointing towards other structures as the root of the problem (Curatolo et al., 2011).

Although many structures and tissues have been explored and sought after for the answer to WAD pathologies, the bulk of the literature has focused on the zygapophysial (facet) joint capsules.

2.5 Evidence for Facet Joint Capsules (FJCs) as a Source of WAD Pain

The facet joints are synovial joints spanning in the transverse plane from the inferior articular process of one vertebra to the superior articular process of the vertebrae directly inferior to it (**Figure 6**). Like most other synovial joints, cervical facet joints are covered in hyaline cartilage and set a joint angle limit at which the joint can safely rotate. Cervical facet joints allow for movement in various planes, however their main function is to allow for, and restrict antero-posterior flexion and extension in the sagittal plane of the neck (Hamill & Knutzen, 2009). The facet joint capsules (FJCs) are known to be a major site of pain for WAD patients through a variety of different methodologies and

techniques, all providing evidence through different perspectives and suggesting similar conclusions (Barnsley, Lord, & Bogduk, 1993; Bogduk, 1999a).

2.5.1 Presence of Nociceptive Innervation

The cervical facet joint receives its sensory innervation via the medial branch of dorsal ramus (Bogduk, 1982). The presence of mechanoreceptive and nociceptive fibres within the FJC has been documented through a variety of staining methods. Using a gold chloride technique, McLain (1994) demonstrated the presence of Type I, II, and III mechanoreceptors in human cervical FJCs. The different types of mechanoreceptors likely respond to different levels of tension, in order to activate protective muscular reflexes (McLain, 1994). In the presence of noxious chemical or physical stimulation, the peripheral endings of nociceptive afferent nerves release substance P (SP) and calcitonin gene-related product peptide (CGRP, Kallakuri et al., 2004). SP and CGRP serve various functions, such as roles in nociception, inflammation, vasoactivity, and tissue repair (Kallakuri et al., 2004). Using an immunohistochemical approach, Kallakuri et al. (2004) demonstrated the presence of these to neuropeptides in human cervical FJCs along with a

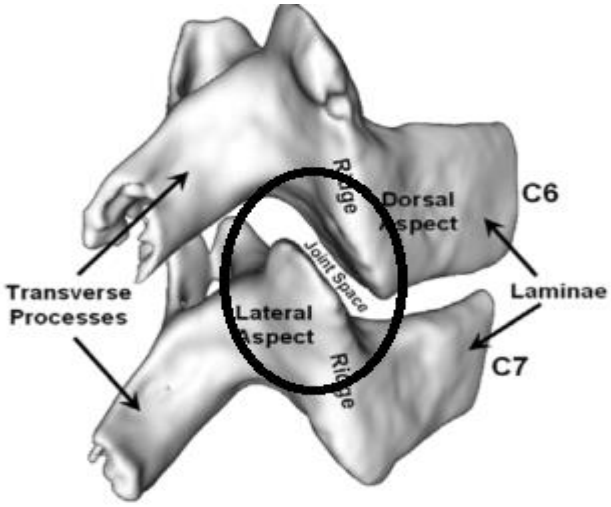

Figure 6: Location of where the facet joint capsule spans across two vertebrae. (Image: adapted from Quinn et al., 2007, p. 5)

pronounced presence of protein gene product 9.5 (a general neuronal marker). The overall presence of these neuropeptides within the FJCs coincides with other studies demonstrating the same fibres at other levels of the vertebral column (Giles & Harvey, 1987; Ashton, Ashton, Gibson, Polak, Jaffray & Eisensten, 1992).

2.5.2 Whiplash-related FJC Injury Mechanism

The human neck response to rear impact has been explored in a number ways including high-speed video camera, accelerometers electromyography and cineradiography (Kaneoka, Ono, Inami, & Hayashi, 1999). Using cineradiography to observe the motion of each cervical vertebra, Kaneoka et al. (1999) had live volunteers accelerate on an impact sled, reaching a velocity of 4 km/hr. Initial neck flexion within the first 100 milliseconds post-collision was observed. This was caused by the forward torso motion forcing C6 to rotate backwards before the upper cervical vertebra, causing the C5-C6 segment's rotational angle to be greater than any other segment at approximately 150 milliseconds. This coincides with what Curatolo et al. (2011) summarized to be the vertebral level most susceptible to a whiplash injury (Kaneoka, et al., 1999). C3-C5 rotational angles increased slowly until approximately 70 milliseconds post-collision, when they accelerated quickly. The creation of the "S"-shape in the cervical spine is consistent with cadaver sled studies (Panjabi et al., 1998; Cusick, Pintar, & Yoganandan, 2001).

Although cineradiography has been used to show joint rotations and translation during simulated collisions, they do not have a high enough resolution to visualize the behaviours of individual structures, especially FJCs (Winkelstein et al., 2000). Studies have used cadaveric whole spines on sled tests to further identify the FJC as a site for

injury from whiplash exposure, as a result of excessive stretch during the whiplash event (Panjabi et al., 1998; Cusick et al., 2001; Pearson et al., 2004). Some sled tests have been shown to replicate similar G-forces to *in vivo* volunteer sled tests and are regarded as favorable alternate options (Cusick et al., 2001). As previously mentioned, the "S"-shaped curve in the cervical spine occurs in the initial stage of the whiplash motion, and that is where the longest elongation of the lower cervical FJCs occurs (Panjabi et al., 1998; Cusick et al., 2001). It is at this point where the FJC is likely to exceed its physiologic strain limit and for injury to occur. Pearson et al. (2004) used established physiologic capsular strain limits (Panjabi, Oxland, Lin, & McGowen 1994) as an indicator for potential injury of the FJC. These limits were exceeded at g-force ranges of 6.5 g and up, confirming those strains as a potential injury mechanism.

Axial pre-torqueing prior to flexion has also been shown to increase capsular strain, including a two-fold increase when the FJC is contralaterally rotated (Winkelstein et al., 2000, Siegmund et al., 2008). These authors suggested that if the head is rotated prior to a whiplash event, there is an increased risk for injury. In addition, axial pre-torque has been shown to create shear strains, directed along the joint line. Strain in this direction has been associated with local sliding of the cervical bony surfaces of the facets (Winkelstein et al., 2000).

2.5.3 Behavioural Evidence

To better understand where the pain may be coming from, and how it arises, quantifying tension in FJCs and observing behavioural responses is the next step. Lee et al. (2004) used an in-vivo rat model to examine whether increasing magnitudes of FJC stretch would elicit pain behaviours. At 300 μm of stretch (the "physiologic vertebral"

level), rats did not exhibit a withdrawal response (i.e., a pain response) to forepaw stimulation. However, at 700 µm of stretch (the "subcatastrophic vertebral" level), the rats exhibited the pain response despite no visible joint failure or tearing having occurred. Winkelstein & Santos (2008) investigated if transection of the facet capsular ligament would also create sustained allodynia. Using a similar in-vivo model, the capsular ligament was stretched to a level where no visible rupture occurred (0.6 mm) but stretched enough to elicit the rats' pain response (paw withdrawal). In another group of rats the FJC was transected, and these rats did not exhibit the pain response. These studies provide behavioural evidence to support FJC stretch as a mechanism of pain.

2.5.4 Neurophysiologic Evidence

A number of studies have demonstrated a link between FJC stretch and activation of neural pathways. Lu, Chen, Kallakuri, Patwardhan, & Cavanaugh (2005a) recorded from the dorsal nerve rootlets during the application of FJC stretch in an in-vivo goat model, and found that the sensory receptors were able to signal a graded mechanical stimulus, which returned to baseline after low-magnitude deformation but persisted for prolonged periods after excessive deformation. Further work has shown different levels of thresholds exist in neural firing (Lu et al., 2005b). Lower threshold units appeared to signal proprioception within the physiological range, and higher, sub-failure threshold strains (35-67%), comparable to those of whiplash (35-60%), likely elicited nociception signals. Additionally, sustained signaling after the initial discharges are hypothesized to contribute to sustained pain sensations (Lu et al., 2005b).

Research at the cellular level has explored the activation of pain sensing fibres in the central nervous system, using an in-vivo a rat model. Quinn, Dong, Golder, &

Winkelstein (2010) reported exaggerated firing responses of neurons in the deep laminae of the dorsal horn across a range of mechanical stimuli, including at sub-failure stretches (no visible signs of tearing) of the FJC. Seven days after the stretching procedure, it was found that the stretched group was more likely to exhibit spontaneous neuronal firing in the dorsal horn than rats in the control group (no stretch). These findings suggest that stretching FJCs with a great enough magnitude to induce mechanical hypersensitivity can also sensitize dorsal horn neurons and cause increased firing to non-noxious and noxious peripheral stimulation. The authors concluded that increased sensitivity in the dorsal horn neurons may drive the mechanical allodynia and hyperalgesia observed in this rat model, and seemed to fall in line with reports from WAD patients (Quinn et al. 2010).

In conjunction with increased sensitivity to dorsal horn neurons, Dong, Odeleye, Jordan-Sciutto, & Winkelstein, 2008 sought to further explore the involvement of the dorsal root ganglion in the event of FJC distraction. The integrated stress response binding protein (BiP) is a marker of endoplasmic reticulum stress response in the dorsal root ganglion, found in the event of injurious stimuli as a protective mechanism by establishing protein homeostasis within the cell (Dong et al., 2008). This study showed that an increased amount of BiP in the dorsal root ganglion was present in rats that underwent a simulated whiplash injury compared to controls. The increase in BiP was also correlated to the mechanical allodynia that was observed the rats 7 days post-operatively. This suggests that there is a relationship between a neuronal response in the dorsal root ganglion and painful FJC injury (Dong et al., 2008).

Another system that has recently been explored in association with pain stemming from the spinal cord after whiplash injuries is the glutamatergic system. Glutamate is a

principal neurotransmitter released by afferent terminals that synapse in the spinal dorsal horn (Dong & Winkelstein, 2010). Two key components of the glutamatergic system that both have crucial roles in chronic pain are the metabotropic glutamate receptor 5 (mGluR5) and the excitatory amino acid carrier 1 (EAAC1) (Dong & Winkelstein, 2010). It is the G protein-coupled receptors that initiate the downstream intracellular signaling, leading to long-term molecular effects of nociceptive modulation, where the mGluR5 specifically increases the excitability of primary afferents and modulates nociceptive neurotransmission of inflammatory pain (Dong & Winkelstein, 2010). On the other hand, excitatory amino acid transporters limit the extracellular concentration of glutamate and prevent over-stimulation of glutamate receptors, yet the EAAC1 in particular is down-regulated after painful peripheral nerve injury (Sung, Lim, & Mao, 2003). Again using rats as a model, Dong & Winkelstein (2010) found that after joint distraction and post-operative mechanical allodynia, there was a significantly higher mGluR5 expression in the spinal cord tissue and significantly reduced amount of EAAC1 compared to a sham group. Based on their findings, Dong & Winkelstein (2010) suggested that the glutamatergic system plays a role in the persistent hypersensitivity of spinal dorsal horn and chronic pain when the FJC undergoes a dynamic whiplash-like loading.

2.5.5 Neuroanatomical Evidence

The axon is a long, thick branch that extends out of the cell body of the neuron, and carries the output signals from smaller, more numerous terminal branches (Latash, 2008). Afferent neurons transmit signals from the periphery to the central nervous system, including pain signals. In the short term, acute pain results from the activation of very thin, unmyelinated C-fibres in the periphery (Winkelstein, 2011). The intention of

nociceptive pain is to protect the tissues, and should only exist while the stimuli are present. In injured tissue, local nociceptors are sensitized; they have an increased firing rate and a lowered threshold for firing when exposed to a previously annoxious stimulus (Kawakami et al., 2003; Rothman & Winkelstein, 2007; Winkelstein, 2011). Tissues eventually heal and neural processes return to normal, however there are cases where pain is persistent and chemical cascades that drive the pain signals become pathologically and permanently altered (Winkelstein, 2011).

Acute and chronic pain can arise from an injury in the peripheral or central nervous system, and is usually located in the part of the body served by the damaged axon (Loeser, 1985). Isolated axons demonstrated a remarkably high tolerance to dynamic stretch injury, experiencing up to 65% strains before showing any sign of impairment (Smith, Wolf, Lusardi, Lee, & Meaney 1999). However, there are some instances where axons may receive extensive damage. In the case where increased strain is applied to the surrounding structures, an early sign of nerve function impairment is a decrease in conduction velocity along the neuron coupled with a decrease in compound action potentials (Smith et al., 1999; Singh, Lu, Chen, Kallakuri, & Cavanaugh, 2006). Povlishock & Christmas (1995) describe two distinct phases of axon injury: primary axotomy, where there is a disruption of the axonal cylinder, and secondary axotomy, where progressive alterations of the axon cylinder take place. Within an hour of a traumatic event, a disturbance triggers an anterograde transport impairment, which creates a block. Despite the block, particles continue to be transported through the axon and once the block is reached, the accumulation of particles will result in axonal swelling (Povlishock & Christman, 1995). The elastic response demonstrated by Smith et al.

(1999) revealed that even though some axons were stretched to 60% their original length at injury; they would return to original length but would begin to show signs of swellings. Kallakuri et al. (2008) confirmed this type of morphology in the event of tensile stretch applied to goat cervical FJCs, demonstrating not only axon swellings (including more than one on the same axon), but also terminal retraction balls, and in some cases excessively knotty, wrinkled and distorted appearances (**Figure 7)**. In the event of an axon transection, which has been shown to happen within 6-12 hours post-injury, the end proximal to the transection is frequently regenerated while the distal segment – no longer attached to the cell body – will degenerate completely and will be removed by tissue macrophages (Junqueira, Carneiro, & Kelley, 1992; Kallakuri et al., 2008).

The majority of laboratory tests of the FJC stretch mechanism for whiplash pain have applied FJC stretch at a low rate. Participant safety is particularly critical in human volunteer studies, to avoid accidentally rupturing the FJC or stretching the FJC beyond

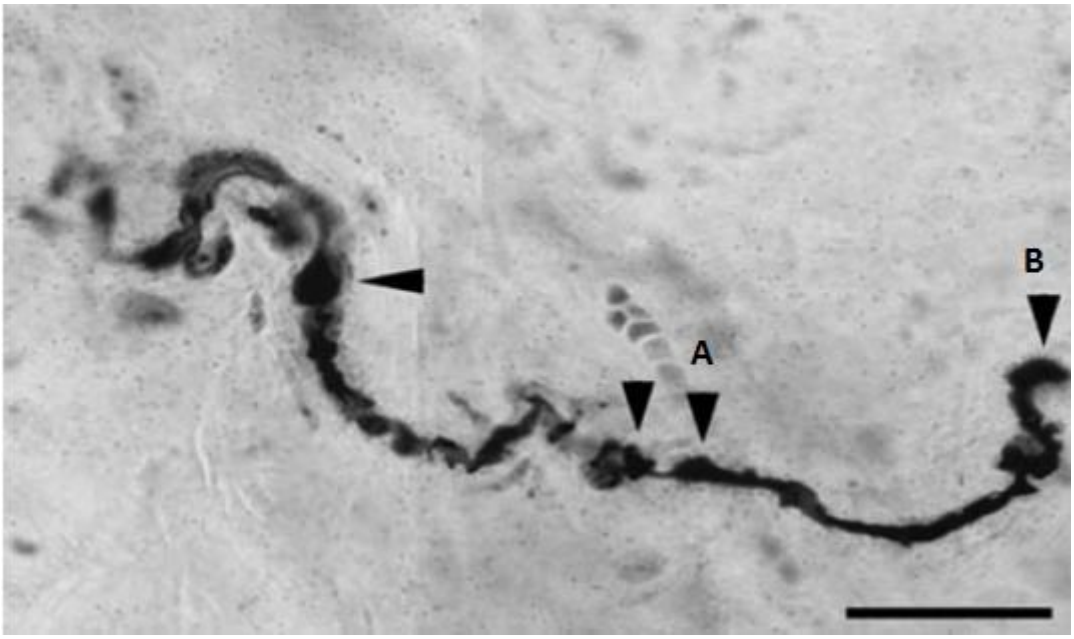

Figure 7: An injured axon showing swellings (A) and retraction balls (B) (arrows). (bar = 20 µm, x100) (Image: adapted from Kallakuri et al., 2008, p. 559).

physiologic range. Therefore, these studies have not been performed at a high rate (Kallakuri et al., 2008; Kaneoka et al., 1999; Winkelstein & Santos, 2008). Furthermore, only a single study has examined stretched FJCs for evidence of axonal injury (Kallakuri et al., 2008), and the FJCs were stretched at a rate of 0.5 mm/s, which more closely represents stretch rates observed in neck motions of activities of daily living (Lu et al., 2005a). In order to more accurately represent the conditions and loading that occur during a whiplash event, high rate stretching of the FJC will be required. To date, no study has examined the axonal changes as a result of high rate tensile stretching of the FJC.

2.6 Cellular Visualization through Immunohistochemistry

Visualizing structures at the microscopic level can prove to be a challenge, given that most tissues are colourless. To overcome this, staining procedures are used to add contrast between the structures to be visualized and the background or other artifacts. Stains are performed using mixtures of dyes or other reagents that stain various tissue components more or less selectively, depending on the type of stain (Junqueira et al., 1992). One method that is commonly employed when visualizing peripheral nervous tissue is immunohistochemistry (IHC). IHC uses antibodies for identifying proteins and molecules in cells and other tissues. This method has been proven to be useful due to the antibodies' highly specific binding to the desired amino acid sequence in proteins (Burry, 2010).

Within the axon, there are integral components that maintain the neuronal structure and aid with the flow of protein in neuronal processes (Friede & Samorajski, 1970). As components of the cytoskeleton of neurons, neurofilament light (NF-L), medium, and heavy chains control the diameter and rate of conduction of the axon

(Schwartz et al., 1998; Van Geel et al., 2005). NF-L is one of the most prominent cytoskeletal components of the neuron, and is capable of organizing into filaments by itself, independent of medium and heavy chains (Carpenter & Ip, 1996; Friede & Samorajski, 1970; Van Geel et al., 2005). In addition, the presence of neurofilament protein outside the axon is considered to reflect neuronal degeneration (Landqvist Waldö, et al., 2013). Thus, NF-L has frequently been used as a target protein for immunolabeling neural structures and has been routinely found either as single fibres or in bundles (Ashton et al., 1992; Inami et al., 2001; Kallakuri et al., 2004, 2012).

Another protein found in nervous tissue is the beta-amyloid precursor protein (β-APP). β-APP is a normal constituent of neuronal cells synthesized in the cytoplasm by the Golgi apparatus and is normally undetectable (Selkoe, 1994; Sherriff, Bridges, & Sivanoganathan, 1994b) The protein is carried along the axon by fast anterograde transport (Koo et al., 1990). In the event of cytoskeletal breakdown, disruptions in axonal transport will occur, where β-APP will accumulate and reach detectable levels (Sherriff, Bridges, Gentleman, Sivaloganathan, & Wilson, 1994a; Uryu, et al., 2007). Antibodies for β-APP have been widely used to detect diffuse axonal injury (An et al., 1997; Gentleman et al., 1993; Hayashi et al., 2009; Sherriff et al., 1994a; Sherriff et al., 1994b; Uryu et al., 2007). There are cases where neurofilament or silver staining may underestimate or misdiagnose axonal injury. In cases where there is short survival time, axon swellings may not have had the time to form, and there may be inconsistencies in the diameter of uninjured axons (Sherriff et al., 1994a; Sherriff et al., 1994b). β-APP accumulation is an energy-requiring process, meaning the injury must occur during life for the accumulation to be detectable, which occurs in as little as three hours (Sherriff et

al, 1994a, Sherriff et al.,1994b). Herein lies the strength of immunolabelling for β-APP: injured axons are labeled specifically and normal axons are not (Hayashi et al., 2009; Sherriff et al., 1994a; Sherriff et al., 1994b; Uryu et al., 2007).

2.7 Summary

In summary, over the past 30 years there has been a continual increase in the prevalence of reported WAD cases, and these injuries create a substantial financial burden on society (Holm et al., 2008). Although the majority of these injuries heal within 3 months after the incident, 14-42% of patients with WAD will progress to chronic symptoms (Barnsley et al., 1994; Gargan & Bannister, 1994; Stovner, 1996; Harder et al., 1998). In Canada, nearly half of the cost of WAD to society is generated by approximately 12% of patients with WAD (Harder et al., 1998).

The whiplash injury mechanism has been shown to be due to abnormal joint rotations in the cervical spine, created by a sigmoid-shape in the cervical spine which appears upon rear-impact (Bogduk, 1999b; Panjabi et al., 1998; Kaneoka et al., 1999; Luan et al., 2000). Within the neck area there are many structures that are possible injury sites for WAD. However, the bulk of the literature strongly suggests that the FJC is the most probable site for injury in a whiplash event. Many approaches have been taken to investigate the FJC's role in WAD pain (e.g., biomechanical, neurophysiological, behavioural, and clinical). From a neuroanatomical perspective, Kallakuri et al. (2008) identified evidence of axonal injury within FJCs exposed to low-rate tensile stretch, but the impact of high-rate tensile stretch on axonal injury has yet to be investigated. IHC's use of antibodies' specificity in identifying desired proteins creates ideal ways to selectively highlight axons in different types of tissues (Burry, 2010). NF-L, being one of

the most prominent cytoskeletal components of the neuron, has frequently been used as a target protein for immunolabeling neural structures (Ashton et al., 1992; Carpenter & Ip, 1996; Inami et al., 2001; Kallakuri et al., 2012). β-APP is another protein found in nervous tissue, and is usually associated with the presence of axonal injury. In the event of cytoskeletal breakdown, β-APP accumulation becomes detectable and because of this has widely been used as a marker of axonal injury (An et al., 1997; Gentleman et al., 1993; Hayashi et al., 2009; Sherriff et al., 1994a; Sherriff, Bridges, & Sivaloganathan, 1994b; Uryu et al., 2007).

CHAPTER 3

Methods

This thesis is part of a larger research program that was conducted in the Department of Biomedical Engineering at Wayne State University, from 2001-2007. Previous studies investigated the neural (Chen, Lu, Cavanaugh, Kallakuri, & Patwardhan, 2005; Lu et al., 2005a, 2005b, 2005c; Chen, Lu, Kallakuri, Patwardhan, & Cavanaugh, 2006) and muscular (Azar, Kallakuri, Chen, Lu, & Cavanaugh, 2009; Azar, Kallakuri, Chen, & Cavanaugh, 2011) responses to facet joint capsule stretch and documented associated FJC axon morphological changes (Kallakuri et al., 2008). Detailed descriptions of the methodologies have been published previously (Azar et al., 2009, 2011; Chen et al., 2005, 2006; Lu et al., 2005a, 2005b, 2005c; Kallakuri et al., 2008). The FJCs used in the present study were harvested during a set of experiments conducted in 2007 (Azar, Kallakuri, Chen, & Cavanaugh, 2011), and have been preserved in 4% buffered paraformaldehyde to prevent tissue degradation. The present study aimed to expand upon what is known with regard to changes in FJC axonal morphology when stretched at a low rate, by examining axonal changes when FJCs are exposed a high-rate stretch, which better simulates the conditions in motor vehicle accidents.

3.1 Test Subjects

Five adult (skeletally mature) Lamancha or Alpine female goats (38-63 kg) were used as human surrogates in this study. For cervical spine studies, goats have shown to be effective in lieu of humans due to their upright head-neck position, which axially loads the cervical spine in a similar fashion to humans (Pintar, Mayer, Yoganandan, & Sun, 2000). It has also been shown that goat and human cervical spines are similar in size,

morphology and alignment of the facet joints (Baisden, Voo, Cusick, Pintar, & Yoganandan, 1999).

3.2 Application of FJC Stretch

3.2.1 Testing Apparatus

A detailed description of the test apparatus construction (**Figure 8**) was provided in Lu et al. (2005c), but a brief description will be provided here. The apparatus consisted of a spine fixator, a stereoimaging system, and an actuator system coupled with a load cell. These components were all fixed to an inverted "T" frame, which was bolted to a steel base frame and secured to the floor to serve as a stationary base. The spine fixator was fastened to the T1 spinous process with a screw, to prevent any unwanted translation during the stretch applications. The goat's neck was elevated so that the C5-C6 joint surface was in line with the horizontal plane (i.e. parallel to the floor). Once the

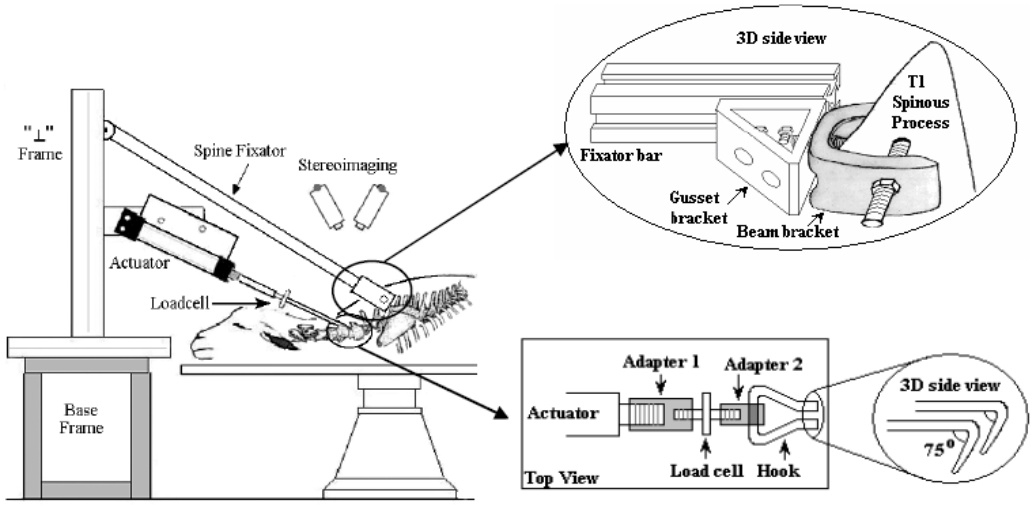

Figure 8: Experimental setup. The goat's spine was held in place by the spine fixator at the T1 spinous process (upper right insert), supported by the inverted "T" frame. The actuator-load cell system was fixed to the inverted "T" frame at one end and to thick, stainless steel wires (2.38 mm diameter) at the other. The wires were bent to create 75° hooks (lower right insert) and inserted to holes drilled into the C5 inferior articular pillar to allow joint distraction (Image: originally published by Lu et al., 2005c, p. 567; adapted by Azar et al, 2009, p. e389).

appropriate position was identified, the adjustable portions of the apparatus were securely locked to anchor the goat spine for mechanical testing of the FJC.

A computer controlled Gemini GV6 digital servo actuator system (Parker Hannifin Corp., Roherk Park, CA, USA) was supported by an aluminium bar fastened perpendicularly to the inverted "T" frame. In order to monitor the tensile stretch, the actuator system was coupled with a 100 lb (444 N) load cell (Entron, Fairfield, NJ, USA). On the distal end of the load cell were two 75° stainless steel hooks (2.38 mm diameter). These hooks were inserted into two holes that were drilled 5 mm apart on the C5 inferior articular process, to apply the tensile stretch.

3.2.2 Surgical Preparation

Azar (2009) provided a full description of the surgical procedures and test protocol, but a brief summary will be provided here. All surgical procedures were reviewed and approved by the Wayne State University Institutional Animal Care and Use Committee (IACUC). After consultation with the head of the University of Windsor's Animal Care Committee (ACC), it was determined that these specimens are considered archival, and further review by the University of Windsor ACC was not required. The goats were anaesthetized throughout the surgical preparation using diazepam (0.5 mg/kg, IM [intramuscular]), pentothal (15 mg/kg, IV [intravenous]), butorphanol (0.22 mg/kg, IM) and atropine (0.066 mg/kg, IM). Maintenance of anesthesia was done via inhalation of isoflurane (2.5-3 %). In the original study, the purpose was to examine the muscle response to the applied stretch of the FJCs. An alternative anaesthetic to isoflurane, which inhibits muscle activity, was required in order to fulfill the primary purpose. Once the surgical preparation was complete, isoflurane was gradually replaced by α-chloralose

for the biomechanical testing, as it does not interfere with muscle activity. α-chloralose was introduced with an initial dose of 60 mg/kg (concentration = 4.16 mg/ml IV) administered over a 20 minute period, and then maintained at a rate of 10-15 mg/kg/hr.

A C2-T2 midline incision was made and the layers of muscle and surrounding tissue were carefully retracted in order to expose the left C5-C6 FJC. In order to allow free movement of the C5 inferior articular process, modifications to the area were required. To create space for the actuator to anchor the C5 inferior articular process, the superior articular process of the same vertebrae was removed. Additionally, the inferior articular process was then trimmed down so that the aforementioned holes (2 mm in diameter, 5 mm apart) could be drilled into the process to allow for the insertion of the hooks. The inferior articular process was then carefully separated from the pedicle without damaging the FJC, yielding a freely moveable C5-C6 FJC (**Figure 9**).

3.2.3 Testing Protocol

Prior to the initiation of the dynamic stretch test series, each FJC was conditioned with 10 cycles of an applied displacement of 1 mm at a rate of 0.5 mm/sec, followed by 10 minutes of rest. The dynamic stretch tests were performed in 4 mm increments of actuator displacement until capsule rupture. The incremental loading paradigm was used in the original study (Azar et al., 2011) so that muscle response could be monitored for several minutes after each FJC stretch. Each test followed a trapezoidal loading pattern consisting of a stretch ramp to the specified displacement (incline of the trapezoid), a 10 second hold (plateau) and a release ramp back to the original position (decline of the trapezoid) (**Figure 10**). In both the stretch phase and release phase, a displacement rate of 100 mm/sec was employed. The purpose of the original study was to monitor the cervical

muscle responses to the applied stretch, thus Azar et al. (2011) spaced each applied displacement by at least 10 minutes to monitor these responses, as well as to reduce the potential of fatigue, muscle potentiation, and reflex habituation (Solomonow, Zhou, Harris, Lu, & Baratta, 1998). Azar et al. (2011) acknowledged that the application of tension over the dorsal aspect of the FJC via joint distraction does not fully mimic the facet joint kinematics during whiplash exposure. Nevertheless, similarities between this protocol and FJC whiplash exposure do exist: the application of tensile stretch via distraction of the joint surfaces (Pearson et al., 2004) at rates comparable to those observed in humans during whiplash exposure (Deng, 1999; Sundararajan, 2005) is consistent with the whiplash mechanism.

3.3 Tissue Harvesting

At the conclusion of the biomechanical testing and neurophysiological recordings, the goats were euthanized by administration of pentothal (90 mg/kg) and bilateral pneumothorax (Azar, 2009). The stretched left C5-C6 (n = 5) and un-stretched right C5-C6 (n = 5) FJCs were carefully harvested using a #10 scalpel blade. The FJCs were then fixed in 4% buffered paraformaldehyde and placed in plastic cassettes until further processing. Fixing the tissues preserves the cellular architecture and composition of cells in the tissue, while also preserving proteins' spatial relationship to the cell so that they can be later studied (Thavarajah, Mudimbaimannar, Elizabeth, Rao, & Ranganathan, 2012). The routinely used 4% formaldehyde is inexpensive and does not cause excessive tissue shrinkage or distortion of cellular structure (Thavarajah et al., 2012).

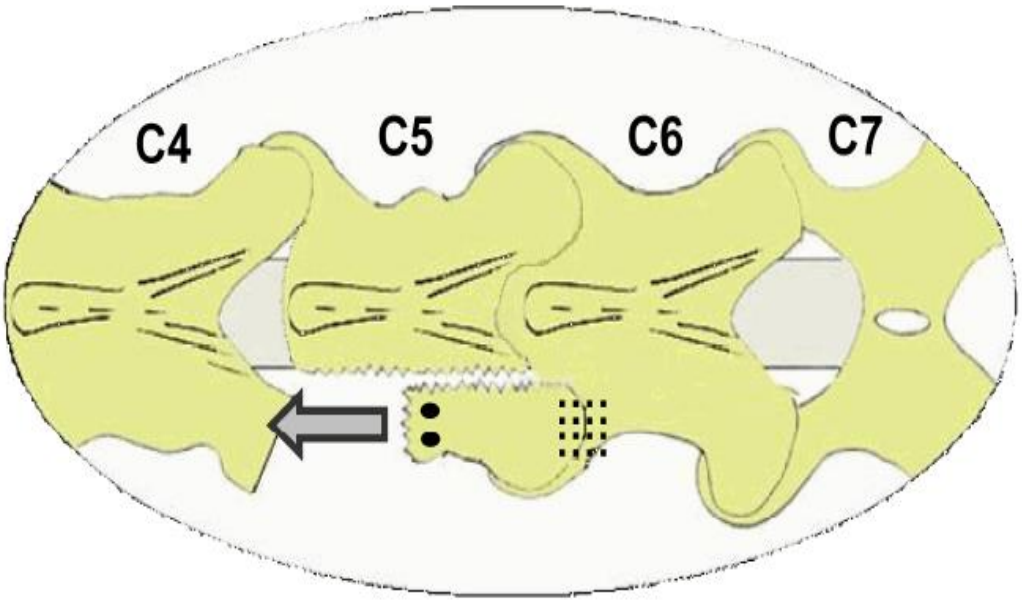

Figure 9: Isolation of C5-C6 FJC for displacement application. In order to create room for joint distraction, the superior articular process of C5 was removed. To freely apply the tensile testing, the C5 inferior articular process was carefully separated from the lamina and pedicle of the C5 vertebrae. Two holes were drilled into the freed process so that the hooks could be inserted to apply the tensile stretch caused by the actuator. The arrow shows the direction of joint distraction applied during the testing (Image: Azar, 2009, p. 33).

3.4 Tissue Integrity Check

Due to the length of time the FJC specimens had been stored in 4% buffered paraformaldehyde, it was critical to determine whether the samples could be immunolabeled to the same degree as fresher tissue. A fresh goat neck was acquired from a local butcher in order to compare the viability of the older preserved tissue against fresh tissue. FJCs of the fresh goat neck were harvested and fixed in 4% buffered paraformaldehyde until further processing. Spinal cord tissue was also harvested from the fresh goat neck to be used as a control in the establishment of proper concentrations of the antibody solutions for the staining procedure. Both original and fresh FJC specimens were prepared and stained under the same conditions, as described below. Upon examination under light microscopy, there was qualitatively very little difference in levels of immunoreactivity between either set of specimens. With both the original and

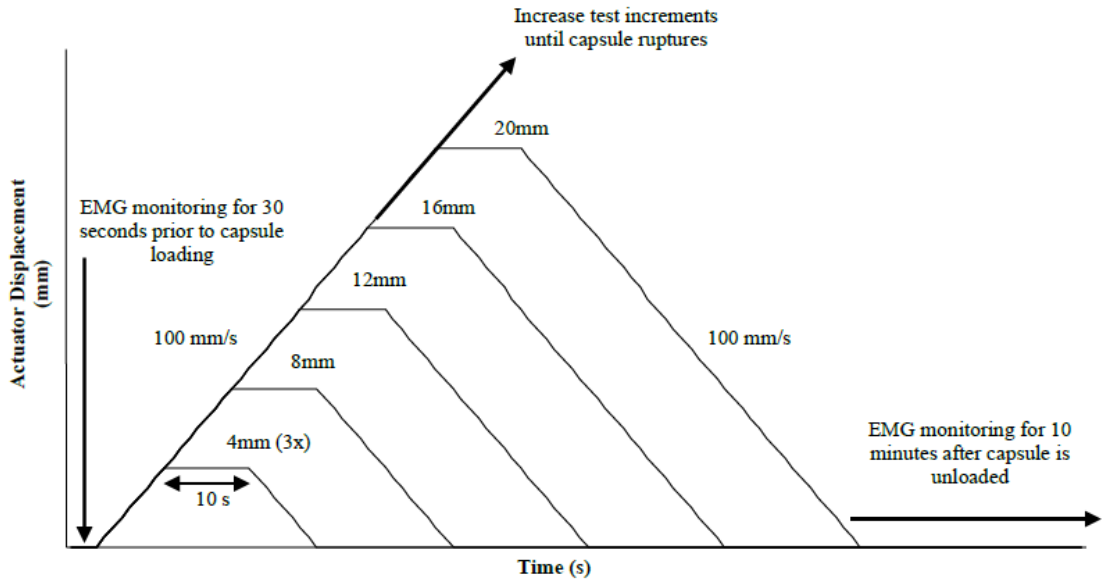

Figure 10: Loading paradigm for dynamic tensile tests. Every joint distraction consisted of the initial pull at 100 m/s followed by a 10 second hold, and then released at 100 m/s. Each test proceeded in 4 mm increments until capsule rupture. In between each test, tensile "re-tests" with a maximum displacement of 4 mm took place (Image: Azar et al., 2011, p. 447).

fresh tissues sharing similar intensity levels of immunoreactivity, confidence was bestowed into achieving reliable staining in the original FJC specimens.

3.5 Tissue Preparation

To protect the tissue and to give it added rigidity during sectioning, the FJCs were embedded into paraffin blocks. The FJCs were thoroughly washed under running tap water and then dehydrated through a graded series of ethyl alcohol baths (70%, 80%, 90%, 100%, 30 minutes each) (UN1170, Decon Laboratories, King of Prussia, PA, USA), which also removed any lingering paraformaldehyde. Following dehydration, the FJCs were cleared with three changes of xylene (class 1C, Fisher X5-500, Thermo Fisher, Waltham, MA, USA). Clearing the tissues in xylene made them more permeable, and allowed more paraffin infiltration to occur. The FJCs were placed in three changes of molten paraffin (50-55°C) and left in a vacuum oven pressurized to 20 inHg, at a temperature of 55°C for 2 hours each change. This removed any air within the tissues and created an ideal environment for maximum paraffin infiltration (the lack of air within the tissue reduces the pressure gradient, thus allowing for easier infiltration of the paraffin). Finally, the tissues were placed into a mold and topped off with paraffin to complete the blocks.

The paraffinized tissues were cut longitudinally in a serial fashion with a width of 10-15 µm. This range of section widths was used in a study of the innervation of the ventral aspect of human cervical FJCs, which employed a similar staining protocol (Kallakuri et al., 2012). The sections were cut using a manual microtome (Reichert Yung, Leica Microsystems Nussloch GmbH, Nussloch). Microscope slides (22265446, Thermo Fisher, MA, USA) were coated in a 1% gelatin solution and left to dry for 30 minutes

before mounting the sections onto them. Coating the slides with 1% gelatin helps the sections adhere more strongly. The sections were cut serially, in ribbons of 2-4 sections, and were mounted serially on the slides.

Immediately prior to staining, the sections were deparaffinized through three changes (2 minutes each) of xylene and rehydrated through graded ethyl alcohol (100%, 90%, 80%, 70%: 2 minutes each) and finally rinsed with tap water.

3.6 Immunohistochemistry

An immunohistochemistry staining approach was chosen to label NF-L and β-APP to show the presence of neurofilaments and detect signs of axonal injury within the FJC, respectively.

3.6.1 Optimization of Antibody Solution Concentration

To achieve the optimal level of immunolabeling (i.e., a balance of sufficient immunoreactivity and minimal background staining), a series of trial immunolabeling was performed to determine the optimal antibody solution concentrations. To attain the appropriate concentration levels, four concentrations (1:500, 1:750, 1:1000, 1:5000) of the primary antibodies were applied to the FJC tissues (NF-L to both original and fresh FJC, β-APP only to original stretched FJC) while maintaining a consistent concentration of 1:500 for the secondary antibody. Upon examination of the four concentrations, 1:1000 was determined to be optimal for both primary antibodies, because at this concentration the axons were clearly discernable from surrounding tissue, and background staining was minimized. To further reduce the level of background staining, the secondary antibody concentration was reduced to 1:1000. A comparison of three

different dilution combinations can be seen in **Figure 11**. Using a 1:1000 concentration for both primary and secondary antibodies provided the desired balance between sufficient immunoreactivity while minimizing the level of background staining.

3.6.2 Positive and Negative Control Procedures

Once the optimal antibody solution concentrations were determined, a series of positive and negative controls were employed to confirm the validity of the antibodies being used in the staining protocol. This was to ensure that the antibodies were labelling what they were supposed to. Solutions of antibodies against NF-L were applied to the FJCs and spinal cord tissue (**Figure 12**) harvested from the fresh goat neck as well as original stretched FJC specimens. β-APP was not expected to label non-injured axons, therefore the control process was only applied to orignal stretched FJC specimens. The spinal cord was used as the positive for this control series due to it being mainly neural tissue, therefore applying antibodies against NF-L to it should label many axons. The process involved following the same protocol, except for the application of primary and/or secondary antibodies. First, both the primary and secondary antibodies were applied to a set of specimens. Another set of specimens was processed with the primary antibody omitted – for this step, the sections were incubated in phosphate buffered saline

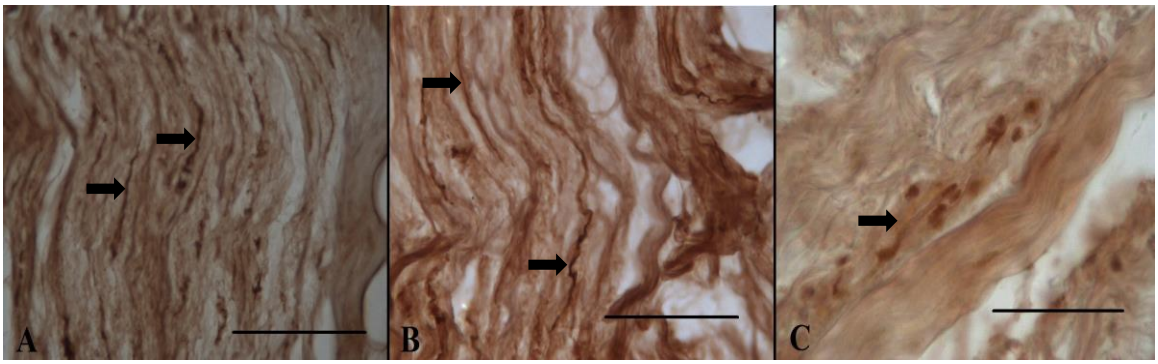

Figure 11: Comparison of three NF-L dilution combinations in original, unstretched FJC [arrows = axons, A: 1° (primary antibody) 1:500, 2° (secondary antibody) 1:500; B: 1° 1:1000, 2° 1:500; C: 1° 1:1000, 2° 1:1000; A & B: 200X, scale bar = 100µm, C: 400X scale bar = 50µm].

(PBS). A third set of specimens was processed with the secondary antibody omitted in favour of PBS. Finally, a fourth set of specimens was processed with both primary and secondary antibodies omitted from the protocol. Only the sections which had both primary and secondary antibodies applied showed sufficient levels of immunoreactivity. Few instances occurred where there was faint immunoreactivity when only the secondary antibody was applied; however, this likely represented non-specific binding, as there were no primary antibodies to bind to. Refer to **Appendix A** for a summary of the control procedure results.

3.6.3 Immunolabeling Procedure

Following deparaffinization, the sections were incubated in PBS until the staining procedure began. Based on previous work in the laboratory, sufficient levels of immunoreactivity have been observed without the use of the citrate buffer step (personal communication, S. Kallakuri, April, 2015). Therefore, this step was omitted throughout the optimization and control procedures. Neglecting this step did not negatively affect

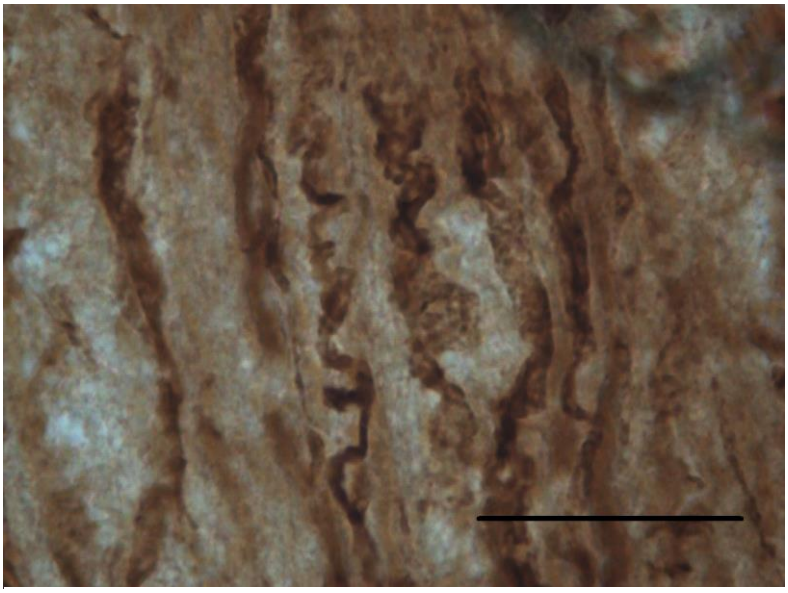

Figure 12: Fresh spinal cord tissue immunolabeled for NF-L (400X, scale bar = 50µm)

levels of immunoreactivity, most likely due to the thinness of the sections. Therefore, the citrate buffer step was removed from the staining protocol. The sections were incubated in 0.3% hydrogen peroxide at room temperature for 60 minutes to block endogenous peroxidase activity. After another series of PBS washes the primary antibody solution (for NF-L: 1:1000 dilution with PBS and 2% normal horse serum, polyclonal anti-goat NF-L raised in rabbit: PA316719, Thermo Fisher Scientific, Waltham, MA, USA. For β-APP: 1:1000 dilution with PBS and 2% normal horse serum, polyclonal anti-goat raised in rabbit: 51-2700, Thermo Fisher Scientific, Waltham, MA, USA), were placed onto the sections and refrigerated at 4°C overnight. Previous authors have confirmed the specificity of the manufacturer's β-APP antibody using Western blot analysis (Nizzari et al., 2007; Stone, Singleton, & Povlishock, 2000). The following day, the primary antibody was collected from the sections and another series of three PBS washes was performed. For both NF-L and β-APP sections, the solution containing the secondary antibodies (1:1000 dilution, biotinylated anti-rabbit IgG raised in horse: BA-1100, Vector Laboratories, Burlingame, CA, USA) was applied to the sections and was left at room temperature for 60 minutes. After another three washes in PBS, the sections were incubated in an avidin-biotin complex (Vectastain Elite ABC reagent, Vector Laboratories, Burlingame, CA, USA) solution for 60 minutes to mark the secondary antibody. Following another series of three PBS washes, a 3,3'-diaminobenzidine (D4293, Sigma Aldrich, St. Louis, MO, USA) solution was applied to each section for five minutes. After three PBS washes the sections were counterstained with hematoxylin for one minute. All sections were washed, dehydrated through graded alcohol (80, 90, 95

& 100%), cleared in xylene and finally fixed to a coverslip with DPX (06522, Sigma Aldrich, St. Louis, MO, USA).

3.7 Imaging

All immunolabeled sections (both stretched and unstretched) were examined under a light microscope (Leica DMLB, Leica Microsystems Ltd, Heerburg, Switzerland). Photomicrographs of all identified neurofibres were taken with a mounted digital camera (Diagnostic Instruments Inc., Sterling Heights, MI, USA).

3.8 Blinded Coding Procedure

A coding procedure involving a singled blinded coder was employed, in order to minimize investigator bias in the identification of immunoreactivity on both NF-L and β-APP labeled sections. One (unblinded) investigator examined each section for possible immunoreactivity. When immunoreactivity was identified, a second investigator who was blind to the condition of the section (stretched vs. unstretched) examined the section and either confirmed or rejected the first investigator's identification.

3.9 Data Analysis

The sections immunolabeled for NF-L were examined first, and sections showing immunoreactivity were noted. β-APP immunolabeled slides were then examined. Upon identification of β-APP immunoreactivity, a check was performed to see if the corresponding NF-L section was also identified as containing immunoreactivity. This was performed to confirm that the β-APP immunoreactivity was highlighting an area that also contained neural tissue. Once a confirmed case of dual immunoreactivity was

identified, those coupled immunoreactive sections were counted as having axonal injury present. In cases where coupled sections contained more than one location with immunoreactivity, that section pair was still only counted as one "injured" section pair.

3.10 Statistical Analysis

Chi-square goodness of fit tests were performed (2 [condition: stretched, unstretched] x 2 [immunoreactivity: positive, negative], $\alpha = 0.05$) using SPSS statistical analysis software (IBM, Armonk, NY, USA). This test was performed to determine if the observed frequencies of confirmed NF-L, β-APP, and coupled NF-L/β-APP immunoreactive sections (respectively) within the stretched and unstretched FJCs were different than expected frequencies. It was expected that a greater number of coupled NF-L/β-APP immunoreactive sections would be observed in the stretched FJCs than in the unstretched FJCs.

CHAPTER 4

Results

From the nine FJCs (5 unstretched, 4 stretched), 180 sections were immunolabeled and examined for immunoreactivity under a light microscope (Leica DMLB, Leica Microsystems Ltd, Heerburg, Switzerland).

4.1 Unstretched FJCs

Forty-eight sections from unstretched FJCs were immunolabeled for NF-L, and each section had a corresponding section that was also immunolabeled for β-APP. Of the 48 sections immunolabeled for NF-L, 19 (39.6%) showed immunoreactivity. Of the 48 sections immunolabeled for β-APP, five (10.4%) showed immunoreactivity; three of these had corresponding sections that were also immunoreactive for NF-L (three out of 48 couples: 6.3%). NF-L immunoreactivity was seen as single or bundles of fibres, typically following a linear path (**Figure 13**).

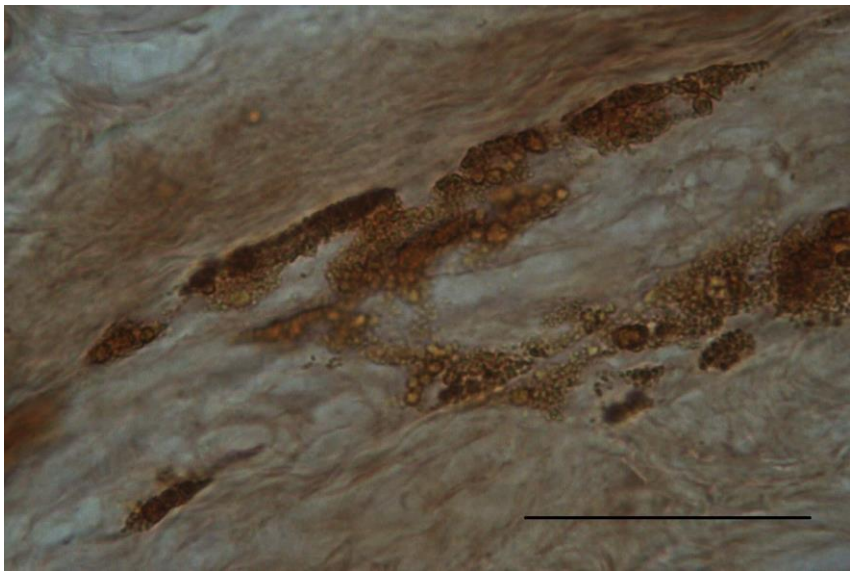

Figure 13: Photomicrograph of NF-L immunoreactivity within an unstretched FJC (400X, scale bar: 50μm).

4.2 Stretched FJCs

Forty-two sections from stretched FJCs were immunolabeled for NF-L, and each section had a corresponding section that was also immunolabeled for β-APP. The rate of positive NF-L immunoreactivity was similar to the unstretched FJCs: 17 sections (40.5%) were NF-L immunoreactive. However, twice as many sections were β-APP immunoreactive in the stretched condition (10 sections out of 42: 23.8%), and all 10 had corresponding sections that were also immunoreactive for NF-L. In the coupled sections, NF-L and β-APP immunoreactivity was identified in similar locations on the sections. In some instances, the stained profiles of neurofibres in corresponding sections were similar in appearance for both stains (**Figure 14**).

4.3 Statistical Analysis

There were no significant deviations from expected frequencies in the observed number of β-APP [X^2 (3, N = 90) = 2.89, p = 0.09, Phi = 0.18: **Table 1**] or NF-L immunoreactive sections [X^2 (3, N = 90) = 0.01, p = 0.93, Phi = 0.009: **Table 2**] between

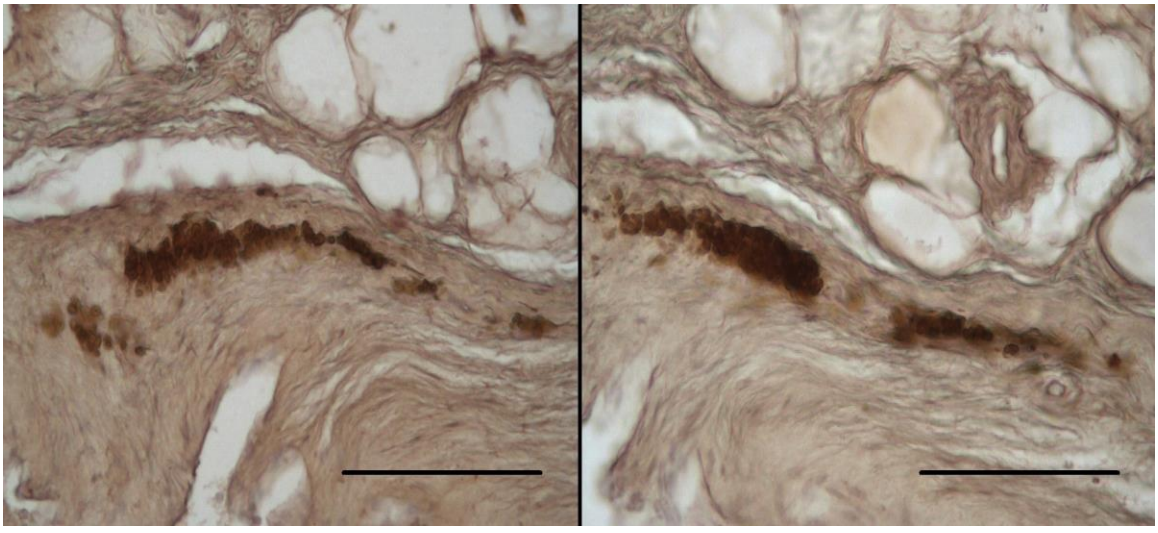

Figure 14: Photomicrographs of the same location on corresponding sections in a stretched FJC (Left: NF-L, Right: β-APP, 200X, scale bar: 100μm).

stretched and unstretched FJCs. There was a significantly higher observed frequency of coupled NF-L/β-APP immunoreactive sections in stretched FJC versus unstretched FJC [X^2 (3, N = 90) = 5.59, p = 0.02, Phi = 0.25: **Table 3**].

Table 1: Frequency counts of β-APP immunolabeled sections by condition.

		Immunoreactivity	
		Positive	Negative
Condition	Stretched	10	32
	Unstretched	5	43

Table 2: Frequency counts of NF-L immunolabeled sections by condition.

		Immunoreactivity	
		Positive	Negative
Condition	Stretched	17	25
	Unstretched	19	29

Table 3: Frequency counts of coupled β-APP/NF-L immunolabeled sections by condition.

		Immunoreactivity	
		Positive	Negative
Condition	Stretched	10	32
	Unstretched	3	45

CHAPTER 5

Discussion

The purpose of this study was to identify axonal injury in goat FJC that were exposed to a high rate tensile stretch in-vivo. The applied stretch rate (100 mm/s) simulated the FJC stretch rates that have been observed in simulations of whiplash events similar to those experienced in a vehicle collision (Deng, 1999; Lu et al., 2005a; Sundararajan, 2005). Immunohistochemical staining was performed to visualize axons within the both stretched and unstretched FJC. The sections were examined for immunoreactivity to NF-L (to identify the presence of axons) and β-APP (to detect axonal injury and distinguish normal from injured axons). NF-L immunoreactivity was observed in 39.6% of the unstretched FJC sections, and in 40.5% in stretched FJC sections. β-APP immunoreactivity was observed in 23.8% of the stretched FJC sections, and these were also positive for NF-L. This was a significantly higher rate of positive immunoreactivity than in the unstretched FJC sections (6.3%, $p = 0.02$). This finding supports the hypothesis of this study, and suggests that high rate tensile stretch is a mechanism for axonal injury within cervical FJC. Using β-APP immunolabeling in combination with NF-L adds strength to these findings, as not only were axons identified (NF-L), injured axons were distinguished from normal axons (β-APP).

NF-L immunolabeling has been routinely used with success to visualize axons across various types of tissues (Friede & Samorajski, 1970; Grady et al., 1993; Dräger & Hofbauer, 1984; Kallakuri et al., 2012; Meller et al., 1993; Schwarz et al., 1998; Van Geel et al., 2005). In the present study, positive NF-L immunoreactivity was identified with similar frequencies across both conditions. This was not surprising given that the

number of axons in each FJC should be relatively similar, and the antibodies for NF-L would label all neurons, whether injured or not. Therefore, observing no significant difference in frequency of positive immunoreactivity between stretched and unstretched FJC suggest that the NF-L immunolabel was consistently successful.

Aside from the specificity of β-APP as a marker for axonal injury, another strength is that the accumulation of β-APP occurs through fast axonal transport and becomes detectable shortly after the initial injury has occurred (Sherriff et al., 1999a, Sherriff et al., 1999b). The speed at which β-APP accumulation occurs was especially relevant for this study, as the goats were sacrificed within approximately 4 hours of the first stretch application and β-APP accumulation, being an energy-requiring process, cannot occur when the goats are not alive. Accumulation of β-APP has been observed to be detectable within the first 3 hours post mortem (Sherriff et al., 1994b), thus the timeframe from the application of FJC stretch to the goats' sacrifice was believed to be long enough to allow β-APP accumulation to occur. When identifying axonal injury based on morphology alone, the post-trauma time period becomes more relevant as the processes of axotomy do not become easily detectable until approximately one hour after trauma (Povlishock & Christman, 1995). Further alterations may take up to 6-12 hours post trauma (Povlishock & Christman, 1995). Therefore, using β-APP immunolabeling leverages β-APP's rapid accumulation to reduce the chances of missing potential axonal injury, as compared to using NF-L and relying on the morphology of axons alone.

Immunolabeling with β-APP has been frequently used to identify axonal injury. However, β-APP immunolabeling has mainly been used in central (brain & spinal cord: An et al. 1997; Gentleman et al., 1993; Hayashi et al., 2009; Sherriff et al. 1994a; Sherriff

et al., 1994b; Uryu et al., 2007) and peripheral (dorsal nerve roots: Singh et al., 2006) neural tissues. This study appears to be the first to use immunoreactivity to β-APP to identify axonal injury in axons embedded in skeletal (i.e., non-neural tissue). It is worth noting that β-APP immunoreactivity was observed in four of the five goats. Having immunoreactivity present in multiple specimens suggests that the injury model was consistent, and that β-APP is an appropriate marker of neuronal injury in this model. This presents an opportunity for further research, especially for injuries and/or diseases that result in axonal injury affecting areas outside of the central nervous system. For example, in certain musculoskeletal injuries such as joint sprains, unidentified neuronal injuries may contribute to pain and joint instability – these would now be able to be identified.

The present study's aim was to expand the knowledge of axonal injury within cervical FJC after being exposed to tensile stretch. Kallakuri et al., (2008) demonstrated the presence of axonal injury in goat cervical FJC after exposure to a low rate tensile stretch. However, the stretch rate they applied (0.5 mm/s) is similar to stretch rates observed in activities of daily living (Lu et al., 2005a), whereas the stretch rate applied in the present study (100 mm/s) more closely replicates whiplash injury conditions occurring in MVA. In their study, Kallakuri et al. (2008) identified abnormal axons by examining their morphology (swellings, terminal retraction balls). Although a blinded multiple-coder procedure was involved to reduce bias, basing results on the appearance of the axons remains somewhat subjective. The dual immunolabeling method used in the present study provided a more objective identification process, because β-APP is not detectable in an uninjured axon. Although the injury identification methods between the two studies were different, a comparison may still be appropriate. In stretched FJC,

Kallakuri et al. (2008) observed that 33.6% of photomicrographs had the presence of abnormal axons, whereas the present study observed that 23.8% of sections showed NF-L/β-APP immunoreactivity. In unstretched FJC, Kallakuri et al (2008) observed that 21.2% of the photomicrographs contained abnormal axons, whereas in the present study, 6.3% dual immunoreactivity was found. It was expected that there would be a higher frequency of axonal injury in the high-rate vs. the low-rate tensile stretch conditions; however, this was not the case. While both studies achieved significant findings; that Kallakuri et al. (2008) found higher frequencies of abnormal axons in both FJC conditions may suggest that using morphology to quantify axonal injury may be subject to overestimation.

The FJC are a known site of pain for WAD patients through a variety of methods: nociceptive innervation (Ashton et al., 1992; Giles & Harvey, 1987; Kallakuri et al., 2004; McLain, 1994), biomechanical evidence (Cusick et al., 2001; Kaneoka et al., 1999; Panjabi et al., 1998; Pearson et al., 2004; Siegmund et al., 2008; Winkelstein et al., 2000), behavioural evidence (Lee et al., 2004; Winkelstein & Stamos, 2008), neurophysiologic evidence (Dong et al., 2008; Dong & Winkelstein, 2010; Lu et al., 2005a; 2005b; Quinn et al., 2010), and neuroanatomical evidence (Junqueira et al., 1992; Kallakuri et al., 2008; Kawakami et al., 2003; Latash, 2008; Loeser, 1985; Povlishock & Christman, 1995; Rotham & Winkelstein, 2007; Singh et al., 2006; Smith et al., 1999; Winkelstein, 2011) all providing converging evidence that the FJC play a significant role in the development of WAD pain (Barnsely et al., 1993; Bogduk, 1999a, Bogduk, 2011). Through a number of histological and immunohistochemical methods (e.g., gold chloride, SP, CGRP, and protein gene product 9.5), the innervation of the cervical FJC has been well documented

(Bogduk, 1982; Kallakuri et al., 2004; McLain, 1994). It may seem intuitive to assume axonal injury occurs at a high-rate stretch if it is present in a lower rate. However, due to the contentious nature of WAD in society, visualizing evidence of axonal injury in FJC exposed to high-rate tensile stretch further implicates the FJC as a source of neck pain in WAD.

5.1 Limitations

The limitations of this study must be addressed. The primary limitation was that this study was a secondary analysis of FJC samples obtained from a larger research program. Although this project was part of the overall research plan, it was not possible to exert as much control over the injury production protocol to optimize it for the specific aims of the present study, which limited the design of the analysis. For example, rather than the incremental stretch paradigm, a single stretch to a particular strain level would have been more representative of the whiplash injury mechanism and its effects on FJC neurons. It also would have allowed the duration of the survival time between stretch application and test subject sacrifice to be better controlled, as some test series ended sooner than others. Although the survival time did exceed the time needed for detectable levels of β-APP to accumulate, an increased length of survival time might have allowed for an increased manifestation of axonal injury in the FJC. Finally, the incremental stretch paradigm also made it impossible to determine exactly when injury occurred. This is because injury likely occurred at a much smaller level than when larger scale ruptures of the FJC became observable. Winkelstein, Nightingale, Richardson, & Myers (1999) observed subcatastrophic failure in tensile tests of human cadaveric FJCs (100 mm/s) at approximately 67% maximal principal strain. This is comparable to the original study

(Azar, 2009), where rupture was visible at 65% maximal principal strain in two of the five capsules. Although this strain level was only reached in two of the five FJC (which may contribute to lower than expected frequency of β-APP immunoreactivity in stretched capsules), it does not discount the possibility of the remaining FJC to have reached strain percentages that yield pain. For example, Lu (2006) observed persistent afterdischarges in group III and IV neurons (slowly-adapting mechanoreceptors) at approximately 28% strain, and in the original study by Azar (2009), persistent cervical muscle afterdischarges (i.e. spasms) were observed at approximately 33% strain. Rupture of the FJC was typically not visible at these strain levels, however the persistent nerve and muscle activity suggests that microdamage may have occurred. These lower strain percentages were reached in four out of the five FJC, indicating that the threshold for potential tissue damage was reached.

A second limitation is the length of time the FJC specimens were stored prior to their use in this study. Ideally, there would be a much smaller time gap between the fixation of the tissue and the time at which the processing and staining of the tissue. Although many efforts were made to determine whether the FJC specimens were still viable, and although the level of immunoreactivity of the original and fresh tissues was comparable, it is still possible that some level of immunoreactivity was lost. This would likely result in an underestimation of the number of immunoreactive sections, thus lowering the frequency counts due to less of the targeted proteins being labeled. This may be another explanation as to why Kallakuri et al. (2008) reported higher frequencies of abnormal axons than the present study. However, since the original and fresh tissues showed similar immunoreactivity, loss of immunoreactivity likely had little impact on the

results. This leads into a future direction of this project where a larger focus is placed on the testing immunoreactivity; going beyond visual observation to quantify differences in immunoreactivity levels between both conditions. This could be done by taking a larger sample size of tissue that has been fixed for a prolonged period of time and comparing frequency counts of immunoreactive sections to tissues has have been fixated for a shorter time period.

In a perfect setting, no β-APP immunoreactivity would be observed in the unstretched FJC, however a small amount of sections indicated potential axonal injury (6.3%). Kallakuri et al. (2008) also identified abnormal axons in unstretched FJC (21.2%). For the present study, it is postulated that undocumented minor injuries to the FJC may have occurred during the goat's life. Another possibility is that the isoflurane anaesthetic used during the surgical protocol may have had some effect in the axons. Xie et al. (2008) have shown that exposure to isoflurane inhalation can result in elevated levels of β-APP in *in vivo* mouse brain, however it's effect on β-APP expression in peripheral neural tissue is unknown. When examining the fresh FJC and spinal cord tissue (which was not subject to any anaesthetic), no β-APP immunoreactivity was present. This suggests that the anaesthetic may have produced some of the axonal injury observed in the test sections, however presence of β-APP immunoreactivity in the unstretched sections was low (6.3%). It is more likely that the unstretched FJC were exposed to unintended perturbations during the surgical preparation and/or testing protocol, or that perhaps small amounts of axonal injury arose from some unknown reason without the need of direct strain or other force applied to the FJC.

Another limitation to this study is that the dual immunolabeling methodology relied on corresponding slides to visualize two different stains at a similar location within the FJC. A potential problem arising from the use of corresponding slides is that there is a chance that the structures captured in one section may no longer exist in the subsequent section. However, due to the thinness of the sections (10-15 μm), the impact of this potential problem was minimized. There were instances where congruent structures were observed through 3-4 adjacent sections. In order to overcome this, future projects may consider a different approach in staining methods. Using immunofluorescent staining to target both NF-L and β-APP on the same section would allow for co-localization to be observed, which may provide further evidence in detecting axonal injury and distinguishing injured from normal axons. Another possible avenue would be an attempt to examine the morphologies of axonal injury through the use of confocal microscopy, where the path of the axon can be better visualized in a third dimension. Furthermore, in the present study all axons with potential axonal injury were identified, but some of these axons may not be involved in pain signaling. A future step could be to determine whether the injured axons were nociceptive fibres or non-nociceptive fibres, through immunofluorescent co-localization of β-APP and pain-related immunolabel targets such as substance P or CGRP.

Investigator bias is a possibility given that a secondary investigator's analysis was only employed upon the identification of possible immunoreactivity by the first investigator. With this method, it is possible that the primary investigator missed potential sites of immunoreactivity. Since the secondary investigator did not analyze the slides independently, these would not have been counted, potentially resulting in an

underestimation of the number of sections showing immunoreactivity. A more suitable identification method would be to have the secondary investigator analyze all of the sections independently from the first primary investigator, and only include sections that were identified as containing immunoreactivity by both investigators in the frequency counts.

This study was conducted using an animal model, which may be problematic due to differences in anatomical dimensions and physiologic responses compared to humans. However, goats have frequently been used as surrogates for cervical spine studies (Azar et al., 2009, 2011; Baisden et al., 1999; Chen et al., 2006; Gu, Jia, & Chen, 2007; Lu et al., 2005a, 2005b, 2005c; Pintar et al., 2000; Zdeblick, Cooke, Wilson, Kunz, & McCabe, 1993), and they are considered an appropriate human surrogate because their upright head-neck position axially loads the cervical spine in a similar fashion to humans (Pintar et al., 2000). Goat necks also share similar cervical spine size, morphology and alignment of FJC, hence findings in *in-vivo* studies can potentially relate to human signs and symptoms (Baisden et al., 1999; Kallakuri et al., 2008).

5.2 Conclusion

The purpose of the study was to identify axonal injury within cervical FJC that were exposed to a high rate tensile stretch. A significantly higher frequency of axonal injury was observed in the stretched FJC, with signs of immunoreactivity appearing in 23.8% of sections versus the 6.3% immunoreactive sections observed in the unstretched capsules. This was the first study to use the combination of NF-L and β-APP immunolabeling to visualize and identify axonal injury in peripheral non-neural tissue. This is significant because it presents a new, viable method for identifying injured axons

embedded within non-neural tissue. The applied rate FJC stretch (100 mm/s) more accurately simulates the FJC loading that would occur during whiplash injuries in MVA scenarios, and this study's findings add to a branch of FJC research that has typically worked with lower rate tensile stretch. The use of a new staining technique, coupled with the high rate tensile stretch condition, furthers the understanding of the role of axonal injury in the developing research of the whiplash pain mechanism.

APPENDIX A

Positive and negative control process. Checkmarks (✓) represent where immunoreactivity was identified, X's represent no immunoreactivity, and the dash (-) represents steps of the process that were not completed due to insufficient tissue. Since the fresh goat neck was not subjected to any injury, and β-APP is a marker for axonal injury, it was not expected to observe any β-APP immunoreactivity in the spinal cord sections.

	Fresh Spinal Cord		Fresh FJC		Original Stretched FJC	
	NF-L	β-APP	NF-L	β-APP	NF-L	β-APP
1° + 2°	✓	X	✓	X	✓	✓
1° only	X	-	X	X	X	X
2° only	X	-	X	X	X	X
Neither	X	-	X	X	X	X

REFERENCES

An, S. F., Giometto, B., Groves, M., Miller, R. F., Beckett, A. A. J., Gray, F., … Scaravilli, F., (1997). Axon damage revealed by accumulation of β-APP in HIV-positive individuals without AIDS. *Journal of Neuropathology and Experimental Neurology, 56*(11), 1262-1268.

Ariëns, G. A. M., van Mechelen, W., Bongers, P. M., Bouter, L. M., van der Wal, G., (2000). Physical risk factors for neck pain. *Scandinavian Journal of Work, Environment & Health, 26*(1), 7-19.

Ashton, I. K., Ashton, B. A., Gibson, S. J., Polak, J. M., Jaffray, D. C., & Eisenstein, S. M. (1992). Morphological basis for back pain: the demonstration of nerve fibers and neuropeptides in the lumbar facet joint capsule but not in ligamentum flavum. *Journal of Orthopaedic Research, 10*(1), 72–78.

Aspden, R. M., (1992). Review of the functional anatomy of the spinal ligaments and the lumbar erector spinae muscles. *Clinical Anatomy 5*, 372-387.

Azar, N. R., Kallakuri, S., Chen, C., & Cavanaugh, J. M. (2011). Muscular response to physiologic tensile stretch of the caprine c5/6 facet joint capsule: dynamic recruitment thresholds and latencies. *Stapp Car Crash Journal, 55*, 441–60.

Azar, N. R., (2009). Muscular response to tensile loading of the cervical facet joint capsule: a potential whiplash pain mechanism (Doctoral Dissertation). Wayne State University, Detroit, MI, USA.

Azar, N. R., Kallakuri, S., Chen, C., Lu, Y., & Cavanaugh, J. M. (2009). Strain and load thresholds for cervical muscle recruitment in response to quasi-static tensile stretch of the caprine C5-C6 facet joint capsule. *Journal of Electromyography and Kinesiology 19*(6), e387–e394.

Baisden, J., Voo, L., Cusick, J., Pintar, F., & Yoganandan, N. (1999). Evaluation of cervical laminectomy and laminoplasty: a longitudinal study in the goat model. *Spine, 24*(13), 1283-1289.

Barnsley, L., Lord, S., & Bogduk, N. (1993). Comparative local anaesthetic blocks in the diagnosis of cervical zygapophysial joint pain. *Pain, 55*(1), 99-106.

Barnsley, L., Lord, S., & Bogduk, N. (1994). Clinical review whiplash injury. *Pain, 58*, 283–307.

Bogduk, N. (1982). The clinical anatomy of the cervical dorsal rami. *Spine, 7*(4), 319-330.

Bogduk, N. (1999a). The neck. *Baillière's Clinical Rheumatology*, *13*(2), 261–285.

Bogduk, N. (1999b). Point of View. *Spine*, *24*(8), 770.

Bogduk, N. (2011). On cervical zygapophysial joint pain after whiplash. *Spine*, *36*(25), S194-S199.

Brault, J. R., Siegmund, G. P., & Wheeler, J. B. (2000). Cervical muscle response during whiplash: evidence of a lengthening muscle contraction. *Clinical biomechanics*, *15*(6), 426-435.

Burry, R. W. (2010). *Immunocytochemistry: a practical guide for biomedical research*. New York: Springer.

Carpenter, D. A., & Ip, W. (1996). Neurofilament triplet protein interactions: evidence for the preferred formation of NF-L-containing dimers and a putative function for the end domains. *Journal of Cell Science*, *109*, 2493-2498.

Chen, C., Lu, Y., Cavanaugh, J. M., Kallakuri, S., & Patwardhan, A. (2005). Recording of Neural Activity From Goat Cervical Facet Joint Capsule Using Custom-Designed Miniature Electrodes. *Spine*, *30*(12), 1367–1372.

Chen, C., Lu, Y., Kallakuri, S., Patwardhan, A., & Cavanaugh, J. M. (2006). Distribution of A-δ and C-fiber receptors in the cervical facet joint capsule and their response to stretch. *The Journal of Bone & Joint Surgery*, *88*(8), 1807-1816.

Chung, Y.-S., & Han, D.-H. (2002). Vertebrobasilar dissection: a possible role of whiplash injury in its pathogenesis. *Neurological Research*, *24*(2), 129–38.

Curatolo, M., Bogduk, N., Ivancic, P. C., McLean, S. A, Siegmund, G. P., & Winkelstein, B. A. (2011). The role of tissue damage in whiplash-associated disorders: discussion paper 1. *Spine*, *36*(25 Suppl), S309–S315.

Cusick, J. F., Pintar, F. A., & Yoganandan, N. (2001). Whiplash Syndrome: Kinematic Factors Influencing Pain Patterns. *Spine*, *26*(11), 1252–1258.

Deng, B., (1999). Kinematics of human cadaver cervical spine during low speed rear-end impacts (Doctoral Dissertation). Wayne State University, Detroit, MI.

Dong, L., Odeleye, A. O., Jordan-Sciutto, K. L., & Winkelstein, B. A. (2008). Painful facet joint injury induces neuronal stress activation in the DRG: Implications for cellular mechanisms of paon. *Neuroscience Letters*, *443*(2), 90–94.

Dong, L., & Winkelstein, B. A. (2010). Simulated whiplash modulates expression of the glutamatergic system in the spinal cord suggesting spinal plasticity is associated with painful dynamic cervical facet loading. *Journal of Neurotrauma*, *27*, 163–174.

Dräger, U. C. & Hofbauer, A. (1984). Antibodies to heavy neurofilament subunit detect a subpopulation of damaged ganglion cells in retina. *Nature, 309*(14), 624-626.

Eichberger, A, Darok, M., & Steffan, H. (2000). Pressure measurements in the spinal canal of post-mortem human subjects during rear-end impact and correlation of results to the neck injury criterion. *Accident Analysis and Prevention, 32*(2), 251–260.

Evans, W. J., Meredith, C. N., Cannon, J. G., Dinarello, C. A, Frontera, W. R., Hughes, V. A, … Knuttgen, H. G. (1986). Metabolic changes following eccentric exercise in trained and untrained men. *Journal of Applied Physiology, 61*(5), 1864–1868.

Francis, C. C. (1955). Dimensions of the cervical vertebrae. *The Anatomical Record, 122*(4), 603-609.

Fredin, Y., Elert, J., Britschgi, N., Nyberg, V., Vaher, A., & Gerdle, B. (1997). A decreased ability to relax between repetitive muscle contractions in patients with chronic symptoms after whiplash trauma of the neck. *Journal of Musculoskeletal Pain, 5*(2), 55–70.

Friede, R. L. & Samorajski, T. (1970). Axon caliber related to neurofilaments and microtubules in sciatic nerve fibers of rats and mice. *The Anatomical Record, 167*(4), 379-387.

Gargan, M., & Bannister, G. (1994). The rate of recovery following whiplash injury. *European Spine Journal, 3*, 162–164.

Gentleman, S. M., Nash., M. J., Sweeting, C. J., Graham, D. I., & Roberts, G. W. (1993). β-Amyloid precursor protein (βAPP) as a marker for axonal injury after head injury. *Neuroscience Letters, 160*, 139-144.

Giles, L. G., & Harvey, A. R. (1987). Immunohistochemical demonstration of nociceptors in the capsule and synovial folds of human zygapophyseal joints. *British Journal of Rheumatology, 26*(5), 362–4.

Grady, M. S., McLaughlin, M. R., Christman, C. W., Valadka, A. B., Fligner, C. L., & Povlishock, J. T., (1993). The use of antibodies targeted against the neurofilament subunits for the detection of diffuse axonal injury in humans. *Journal of Neuropathology and Experimental Neurology, 52*(2), 143-152.

Gray, H., & Lewis, W. (2000). *Anatomy of the human body*. Bartleby.com.

Gu, Y. -T., Jia, L. -S., & Chen, T. -Y. (2007). Biomechanical study of a hat type cervical intervertebral fusion cage. *International Orthopaedics, 31*, 101-105.

Hamill, J., & Knutzen, K. (2009). *Biomechanical basis of human movement* (3rd ed.). Philadelphia: Lippincott Williams & Wilkins.

Harder, S., Veilleux, M., & Suissa, S. (1998). The effect of socio-demographic and crash-related factors on the prognosis of whiplash. *Journal of clinical epidemiology*, *51*(5), 377-384.

Hayashi, T., Ago, K., Ago, M., & Ogata, M. (2009). Two patterns of β-amyloid precursor protein (APP) immunoreactivity in cases of blunt head injury. *Legal Medicine, 11,* S171-S173.

Hogg-Johnson, S., van der Velde, G., Carroll, L. J., Holm, L. W., Cassidy, J. D., Guzman, J., … Peloso, P. (2008). The burden and determinants of neck pain in the general population: results of the Bone and Joint Decade 2000–2010 Task Force on Neck Pain and Its Associated Disorders. *European Spine Journal, 17*(S1), S39–S51.

Holm, L. W., Carroll, L. J., Cassidy, J. D., Hogg-Johnson, S., Côté, P., Guzman, J., … Haldeman, S. (2008). The Burden and Determinants of Neck Pain in Whiplash-Associated Disorders After Traffic Collisions. *European Spine Journal, 17*(S1), 52–59.

Inami, S., Shiga, T., Tsujino, A., Yabuki, T., Okado, N., & Ochiai., N. (2001). Immunohistochemical demonstration of nerve fibers in the synovial folds of the human cervical facet joint. *Journal of Orthopaedic Research, 19,* 593-596.

Junqueira, L., Carneiro, J., & Kelley, R. (1992). *Basic Histology* (7th ed., pp. 163-188). East Norwalk: Prentice-Hall International.

Kallakuri, S., Li, Y., Chen, C., & Cavanaugh, J. M. (2012). Innervation of cervical ventral facet joint capsule: Histological evidence. *World Journal of Orthopedics*, *3*(2), 10–14.

Kallakuri, S., Singh, A., Chen, C., & Cavanaugh, J. M. (2004). Demonstration of substance P, calcitonin gene-related peptide, and protein gene product 9.5 containing nerve fibers in human cervical facet joint capsules. *Spine*, *29*(11), 1182–1186.

Kallakuri, S., Singh, A., Lu, Y., Chen, C., Patwardhan, A., & Cavanaugh, J. M. (2008). Tensile stretching of cervical facet joint capsule and related axonal changes. *European Spine Journal*, *17*, 556–563.

Kamibayashi, L. K. & Richmond, F. J. R. (1998). Morphometry of human neck muscles. *Spine, 23*(12), 1314-1323.

Kawakami, M., Hashizume, H., Nishi, H., Matsumoto, T., Tamaki, T., & Kuribayashi, K. (2003). Comparison of neuropathic pain induced by the application of normal and mechanically compressed nucleus pulposus to lumbar nerve roots in the rat. *Journal of Orthopaedic Research, 21*, 535-539.

Kaneoka, K., Ono, K., Inami, S., & Hayashi, K. (1999). Motion Analysis of Cervical Vertebrae During Whiplash Loading. *Spine*, *24*(8), 763–770.

Koo, E. H., Sisodia, S. S., Archer, D. R., Martin, L. J., Weidemann, A., Beyreuther, K., … Price, D. L. (1990). Precursor of amyloid protein in Alzheimer disease undergoes fast anterograde axonal transport. *Proceedings of the National Academy of Sciences of the United States of America*, *87*(4), 1561–1565.

Landqvist Waldö, M., Frizell Santillo, A., Passant, U., Zetterberg, H., Rosengren, L., Nilsson, C., & Englund, E. (2013). Cerebrospinal fluid neurofilament light chain protein levels in subtypes of frontotemporal dementia. *BMC Neurology, 13*(54), 1-8.

Lee, K., Thinnes, J., Gokhin, D., & Winkelstein, B. A. (2004). A novel rodent neck pain model of facet-mediated behavioral hypersensitivity: implications for persistent pain and whiplash injury. *Journal of Neuroscience Methods*, *137*(2), 151–159.

Loeser, J. D. (1985). Pain due to nerve injury. *Spine*, *10*(3), 232-235.

Lu, Y. (2006). Neural response of the cervical facet joint capsule stretch: a potential whiplash pain mechanism (Doctoral Dissertation). Wayne State University, Detroit, MI.

Lu, Y., Chen, C., Kallakuri, S., Patwardhan, A., & Cavanaugh, J. M. (2005a). Neurophysiological and biomechanical characterization of goat cervical facet joint capsules. *Journal of Orthopaedic Research, 23*, 779-787.

Lu, Y., Chen, C., Kallakuri, S., Patwardhan, A., & Cavanaugh, J. M. (2005b). Neural response of cervical facet joint capsule to stretch: a study of whiplash pain mechanism. *Stapp Car Crash Journal*, *49*, 1-17.

Lu, Y., Chen, C., Kallakuri, S., Patwardhan, A., & Cavanaugh, J. M. (2005c). Development of an in vivo method to investigate biomechanical and neurophysiological properties of spine facet joint capsules. *European Spine Journal*, *14*(6), 565–72.

Luan, F., Yung, K. H., Deng, B., Begeman, P. C., Tashman, S., & King, A. I. (2000). Qualitative analysis of neck kinematics during low-speed rear-end impact. *Clinical Biomechanics*, *15*, 649-657.

McLain, R. F. (1994). Mechanoreceptor endings in human cervical facet joints. *Spine, 19*(5), 495-501.

Meller, D., Bellander, B. -M., Schmidt-Kastner, R., & Ingvar, M. (1993). Immunohistochemical studies with antibodies to neurofilament proteins on axonal damage in experimental focal lesions in rat. *Journal of the Neurological Sciences, 117*, 164-174.

Mosby's dictionary of medicine, nursing and health professions (9th ed.). (2013). St Louis, MO: Elsevier/Mosby.

Navin, F., Zein, S., & Felipe, E. (2000). Road safety engineering: an effective tool in the fight against whiplash injuries. *Accident Analysis and Prevention, 32*, 271-275.

Nizzari, M., Venezia, V., Repetto, E., Caorsi, V., Magrassi, R., Galiani, M. C., … Russo, C. (2007). Amyloid precursor protein and presenilin1 interact with the adaptor GRB2 and modulate ERK1,2 signaling. *The Journal of Biological Chemistry, 282*(18), 13833-13844.

Panjabi, M. M., Cholewicki, J., Nibu, K., Grauer, J. N., Babet, L. B., & Dvorak, J. (1998). Mechanism of whiplash injury. *Clinical Biomechanics, 13*, 239-249.

Panjabi, M. M., Duranceau, J., Goel, V., Oxland, T., & Takata, K. (1991a). Cervical human vertebrae: quatitative three-dimensional anatomy of the middle and lower regions. *Spine, 16*(8), 861-869.

Panjabi, M. M., Oxland, T. R., & Parks, E. H. (1991b). Quantitative anatomy of cervical spine ligaments. Part II. Middle and lower cervical spine. *Journal of Spinal Disorders, 4*(3), 277-285.

Panjabi, M. M., Oxland, T. R., Lin, R., & McGowen, T. W (1994). Thoracolumbar burst fracture: a biomechanical investigation of its multidirectional flexibility. *Spine, 19*(5), 578-585.

Pearson, A., Ivancic, P., Ito, S., & Panjabi, M. (2004). Facet joint kinematics and injury mechanisms during simulated whiplash. *Spine, 29*(4), 390–7.

Pintar, F., Mayer, R., Yoganandan, N., & Sun, E. (2000). Child neck strength characteristics using an animal model. *Stapp Car Crash Journal, 44*, 77-83.

Povlishock, J. T. & Christman, C. W. (1995). The pathobiology of traumatically induced axonal injury in animals and humans: a review of current thoughts. *Journal of Neurotrauma, 12*(4), 555-564.

Quinn, K. P., Dong, L., Golder, F. J., & Winkelstein, B. A. (2010). Neuronal hyperexcitability in the dorsal horn after painful facet joint injury. *Pain, 151*(2), 414–421.

Quinn, K. P., Lee, K. E., Ahaghotu, C. C., & Winkelstein, B. A. (2007). Structural changes in the cervical facet capsular ligament : potential contributions to pain following subfailure loading. *Stapp Car Crash Journal, 51*(October), 1–19.

Rothman, S. M. & Winkelstein, B. A. (2007). Chemical and mechanical nerve root insults induce differential behavioral sensitivity and glial activation that are enhanced in combination. *Brain Research, 1181*, 30-43.

Scholten-Peeters, G. G., Verhagen, A. P., Bekkering, G. E., van der Windt, D. A., Barnsley, L., Oostendorp, R. A., & Hendriks, E. J. (2003). Prognostic factors of whiplash-associated disorders: a systematic review of prospective cohort studies. *Pain, 104*(1), 303-322.

Schulte, E., Schuenke, M., & Schumacher, U. (2006). Neurovascular structures. In *Atlas of Anatomy: Neck and Internal Organs,* (1st ed., pp. 16-17). Stuttgart: Thieme.

Schwartz, M. L., Hua, Y., Cañete-Soler, R., & Schlaepfer, W. W. (1998). Characterization of the mouse neurofilament light (NF-L) gene promoter by in vitro transcription. *Molecular Brain Research, 57*, 21-30.

Scott, S., & Sanderson, P. L. (2002). Whiplash: a biochemical study of muscle injury. *European Spine Journal, 11*, 389–92.

Selkoe, D. J. (1994). Normal and abnormal biology of the beta-amyloid precursor protein. *Annual Review of Neuroscience, 17*, 489-517.

Šerić, V., Blažić-Čop, N., & Demarin, V. (2000). Haemodynamic changes in patients with whiplash injury measured by transcranial Doppler sonography (TCD). *Collegium Antropologicum, 24*(1), 197–204.

Sherriff, F. E., Bridges., L. R., Gentleman, S. M., Sivaloganathan, S. & Wilson, S. (1994a). Markers of axonal injury in post mortem human brain. *Acta Neuropathologica, 88*, 433-439.

Sherriff, F. E., Bridges, L. R., & Sivaloganathan, S. (1994b). Early detection of axonal injury after human head trauma using immunocytochemistry for β-amyloid precursor protein. *Acta Neuropathologica, 87*, 55-62.

Shi, S. R., Chaiwun, B., Young, L., Cote, R. J., & Taylor, C. R. (1993). Antigen retrieval technique utilizing citrate buffer or urea solution for immunohistochemical demonstration of androgen receptor in formalin-fixed paraffin sections. *Journal of Histochemistry & Cytochemistry, 41*(11), 1599-1604.

Siegmund, G. P., Davis, M. B., Quinn, K. P., Hines, E., Myers, B. S., Ejima, S.,… Winkelstein, B. A., (2008). Head-turned postures increase the risk of cervical facet capsule injury during whiplash. *Spine, 33*(15), 1643-1649.

Siegmund, G. P., Sanderson, D. J., Myers, B. S., & Inglis, J. T. (2003). Awareness affects the response of human subjects exposed to a single whiplash-like perturbation. *Spine, 28*(7), 671-679.

Singh, A., Lu, Y., Chen, C., Kallakuri, S., & Cavanaugh, J. M. (2006). A new model of traumatic axonal injury to determine the effects of strain and displacement rates. *Stapp Car Crash Journal, 50*, 601-623.

Skandalakis, J. E., Colburn, G. L., Weidman, T. A., Foster Jr, R. S., Kingsworth, A. N., Skandalakis, L. J.,… Mirilas, P. S. (2004) *Skandalakis' Surgical Anatomy: The embryologic and anatomic basis of modern surgery.* Athens, Greece: Paschalidis Medical Publications, Ltd.

Smith, D. H., Wolf, J. A., Lusardi, T. A., Lee, V. M.-Y., & Meaney, D. F. (1999). High tolerance and delayed elastic response of cultured axons to dynamic stretch injury. *The Journal of Neuroscience, 19*(11), 4263-4269.

Solomonow, M., Zhou, B.-H., Harris, M., Lu, Y., & Baratta, R. V. (1998). The ligamento-muscular stabilizing system of the spine. *Spine*, *23*(23), 2552–2562.

Stone, J. R., Singleton, R. H., & Povlishock, J. T. (2000). Antibodies to the C-terminus of the β-amyloid precursor protein (APP): a site specific marker for the detection of traumatic axonal injury. *Brain Research, 871*, 288-302.

Stovner, L. J. (1996). The nosologic status of the whiplash syndrome: a critical review based on a methodological approach. *Spine*, *21*(23), 2735-2746.

Sundararajan, S. (2005). Effect of head-neck position on cervical facet stretch of post mortem human subjects during low speed rear end impacts (Doctoral Dissertation). Wayne State University, Detroit, MI.

Sung, B., Lim, G., & Mao, J. (2003). Altered expression and uptake activity of spinal glutamate transporters after nerve injury contribute to the pathogenesis of neuropathic pain in rats. *The Journal of Neuroscience, 23*(7), 2899-2910.

Svensson, M. Y., Aldman, B., Boström, O., Davidsson, J., Hansson, H. A., Lövsund, P., ... & Säljö, A. (1998). Nerve cell damages in whiplash injuries. Animal experimental studies. *Der Orthopade*, *27*(12), 820-826.

Taneichi, H., Suda, K., Kajino, T., & Kaneda, K. (2005). Traumatically induced vertebral artery occlusion associated with cervical spine injuries: prospective study using magnetic resonance angiography. *Spine, 30*(17), 1955–62.

Thavarajah, R., Mudimbaimannar, V. K., Elizabeth, J., Rao, U. K., & Ranganathan, K. (2012). Chemical and physical basics of routine formaldehyde fixation. *Journal of Oral and Maxillofacial Pathology, 16*(3), 400-405.

Tortora, G. J., & Nielsen, M. T. (2009). *Principles of Human Anatomy* (11th ed., pp. 197-199). Hoboken: John Wiley & Sons.

Uryu, K., Chen, X. H., Martinez, D., Browne, K. D., Johnson, V. E., Graham, D. I., … Smith., D. H. (2007). Multiple proteins implicated in neurodegenerative diseases accumulate in axons after brain trauma in humans. *Experimental Neurology, 208*, 185-192.

Van Geel, W. J. A., Rosengren, L. E., Verbeek, M. M. (2005). An enzyme immunoassay to quantify neurofilament light chain in cerebrospinal fluid. *Journal of Immunological Methods, 296*, 179-185).

Winkelstein, B. A. (2011). How can animal models inform on the transition to chronic symptoms in whiplash? *Spine, 36*(25 Suppl), S218–25.

Winkelstein, B. A., McLendon, R. E., Barbir, A., & Myers, B. S. (2001). An anatomical investigation of the human cervical facet capsule, quatifying muscle insertion area. *Journal of Anatomy, 198*(4), 455-461.

Winkelstein, B. A., Nightingale, R. W., Richardson, W. J., & Myers, B. S., (1999). Cervical facet joint mechanics: its application to whiplash injury. In Proceedings of the 43rd Stapp Car Crash Conference. San Diego, CA. SAE Paper # 99SC15.

Winkelstein, B. A., Nightingale, R. W., Richardson, W. J., & Myers, B. S. (2000). The cervical facet capsule and its role in whiplash injury: a biomechanical investigation. *Spine*, *25*(10), 1238–46.

Winkelstein, B. A., & Santos, D. G. (2008). An intact facet capsular ligament modulates behavioral sensitivity and spinal glial activation produced by cervical facet joint tension. *Spine*, *33*(8), 856–62.

Xie, Z., Culley, D. J., Dong, Y., Zhang, G., Zhang, B., Moir, R. D., Frosch, M. P., Crosby, G., & Tanzi, R. E. (2008) The common inhalation anesthetic isoflurane induces caspase activation and increases amyloid β-protein level in vivo. *Annals of Neurology*, *64*(6), 618-627.

Yoganandan, N., Cusick, J., Pintar, F., & Rao, R. (2001). Whiplash injury determination with conventional spine imaging and cryomicrotomy. *Spine*, *26*(22), 2443–8.

Zdeblick, T. A., Cooke, M. E., Wilson, D., Kunz, D. N., & McCabe, R. (1993). Anterior cervical discectomy, fusion and plating: a comparaitve animal study. *Spine, 18*(14), 1974-1983.

VITA AUCTORIS

NAME:	Christopher Shaw
PLACE OF BIRTH:	Ottawa, ON
YEAR OF BIRTH:	1990
EDUCATION:	St. Peter Catholic High School, Ottawa, ON, 2008
	University of Windsor, B.H.K., Windsor, ON, 2012